Dissecting durum wheat time to anthesis into physiological traits using a QTL-based model

Pierre Martre, Rosella Motzo, Anna Maria Mastrangelo, Daniela Marone, Pasquale De Vita, Francesco Giunta

European Journal of Agronomy 161 (2024) 127379

Contents lists available at ScienceDirect

European Journal of Agronomy

journal homepage: www.elsevier.com/locate/eja

Dissecting durum wheat time to anthesis into physiological traits using a QTL-based model

Pierre Martre [a,*,1], Rosella Motzo [b,2], Anna Maria Mastrangelo [c,3], Daniela Marone [c,4], Pasquale De Vita [c,5], Francesco Giunta [b]

[a] LEPSE, Univ. Montpellier, INRAE, Institut Agro Montpellier, Montpellier, France
[b] Unit of Agronomy, Field Crops and Genetics, Department of Agriculture, University of Sassari, Sassari, Italy
[c] CREA, Research Centre for Cereal and Industrial Crops, Foggia, Italy

ARTICLE INFO

Keywords:
Crop model
Durum wheat
Genotype-to-phenotype modeling
Phenology
Phyllochron
QTL-based model

ABSTRACT

Fine tuning crop development is a major breeding avenue to increase crop yield and for adaptation to climate change. We used an ecophysiological model that integrates our current understanding of the physiology of wheat phenology to predict the development and anthesis date of 91 recombinant inbreed lines (RILs) of durum wheat with genotypic parameters controlling vernalization requirement, photoperiod sensitivity, and earliness *per se* estimated using leaf stage, final leaf number, anthesis date data from a pot experiment with vernalized and nonvernalized treatments combined with short- and long-day length. Predictions of final leaf number and anthesis date of the QTL-based model was evaluated for the whole population of RILs in a set of independent field trials and for the two parents, which were not used to estimate the parameter values. Our novel approach reduces the number of environments and the time required to obtain the required data sets to develop a QTL-based prediction of model parameters. Moreover, the use of a physiologically based model of phenology gives new insight into genotype-phenology relations for wheat. We discuss the approach we used to estimate the parameters of the model and their association with QTL and major phenology genes that collocate at QTL.

1. Introduction

The increase in the occurrence and intensity of drought and heat stress due to global climate change is accompanied by a greater impact of genotype by environment interactions (G x E) on crop yields (Xiong et al., 2021), making breeding for adaptation more difficult. A fine-tuning of plant development is an avenue to cope with future climates and weather variability. Plant development is an important determinant of G x E and climate adaptation (Asseng et al., 2019; Fischer, 2016; Parent et al., 2018) and large and well understood genetic variations in vernalization, photoperiod sensitivity, and earliness *per se*, the three components of crop earliness, is available to crop breeders (Hyles et al., 2020; Kiss et al., 2017).

Ecophysiological models are powerful tools to get a better insight into how G x E interactions come about and to predict the performance of genotypes in defined environments (e.g. Bertin et al., 2010), although it requires more robust and biological sound crop models than do conventional agricultural applications (Hammer et al., 2019). Phenology models can be classified in two groups according to how they simulate development. The classical approach is based on accumulated thermal time between development phases modified by photoperiod and/or vernalization status of the plants. Alternately, a physiological approach dissects time to anthesis into primordium, leaf production, and leaf growth processes, which integrate the effects of vernalization and photoperiod (He et al., 2012; Jamieson et al., 1998). These two approaches can give similar predictions of anthesis date (Jamieson et al., 2007). However, the advantage of a physiological-based approach to dissect flowering time into component traits goes beyond the capability

* Correspondence to: INRAE – UMR LEPSE, 2 place Pierre Viala, Montpellier 34060, France.
E-mail address: pierre.martre@inrae.fr (P. Martre).
[1] 0000-0002-7419-6558
[2] 0000-0002-0407-6622
[3] 0000-0002-3618-0301
[4] 0000-0002-2365-6091
[5] 0000-0002-9573-0510

https://doi.org/10.1016/j.eja.2024.127379
Received 16 January 2024; Received in revised form 22 July 2024; Accepted 29 September 2024
Available online 10 October 2024

to simulate anthesis date by establishing a strong physiological link between phenotype and genotype (Brown et al., 2013).

The structure of a model and the way interactions between the underlying processes are considered is essential to model genetic variability (Parent and Tardieu, 2014). To correctly simulate G x E, model architecture and associated coefficients should capture and integrate the physiological basis of the genetic variations. The physiological-based approach to model plant development has a greater potential explanatory capability of G x E because it simulates the avenues by which each genotype reaches anthesis. Whether the same anthesis date is reached by two different genotypes through less leaves or through a faster rate of leaf appearance is likely to affect genotype adaptation, not only through time to anthesis, but also via processes like leaf growth and final leaf size (Dornbusch et al., 2011), tiller production and mortality (Giunta et al., 2018) or ear fertility (Gonzalez-Navarro et al., 2016; Ochagavía et al., 2018, 2017). The physiological approach to model phenology allows linking phenology with leaf area and tillering and to analyze interactions and trade-offs between these processes (Abichou et al., 2018; Martre and Dambreville, 2018).

Previous studies linked crop phenology model parameters with known phenology genes Hoogenboom and White, (2003), Hoogenboom et al., (1997), for common bean; White et al. (2008), for winter wheat; Zheng et al. (2013), for spring wheat) or by identifying quantitative trait loci (QTL) associated with model parameters (Bogard et al. (2020a), for spring wheat; Bogard et al. (2014), for winter wheat; Nakagawa et al. (2005), for rice; Yin et al. (2005), for spring barley). All these studies have used phenology models based on accumulated thermal time between growth phases that do not consider leaf development. 'Genetic' parameters of the models were estimated together using observations of heading or anthesis date, which imply a long phenotypic distance between the observed variables and the model parameters.

In this study we developed a QTL-based model based on the phenological framework proposed by Jamieson et al. (1998) to predict leaf development and anthesis date of a recombinant inbreed line (RIL) population of durum wheat (*Triticum turgidum* L. subsp. *durum* (Desf.) Husn.). In contrast with previous studies, we estimated the parameters controlling vernalization requirement, photoperiod sensitivity, and earliness *per se* for each genotype separately using leaf stage, final number, anthesis date data from a pot experiment with vernalized and nonvernalized treatments combined with short- and long-day length. QTL associated with each of the five genetic parameters of the model were used to obtain multiple linear regression prediction of the parameter values. Predictions of final leaf number and anthesis date of the QTL-based model was evaluated for the whole population of RILs in a set of independent field trials and for the two parents, which were not used to estimate the parameter values. Compared with the classically approach, which uses muti-year and multi-site field trials, our approach, which requires only three experimental treatments that can be carried out in the same year, reduces the number of environments, and the time required to obtain the required data sets to develop a QTL-based prediction of model parameters. The use of a physiologically based model of phenology gives new insight into genotype-phenology relations for wheat. Several of the QTL associated with model parameters co-localized with known vernalization requirement and photoperiod sensitivity genes or QTL.

2. Materials and methods

2.1. Plant materials

Ninety-one lines of a F2-derived, F8-F9 recombinant inbred lines (RILs) mapping population obtained from a cross between the Italian durum wheat (*Triticum turgidum* L. subsp. *durum* (Desf.) Husn.) cultivars Ofanto and Cappelli were used (Verlotta et al., 2010). Ofanto is an early flowering, semi-dwarf cultivar released in 1990 that originated from a cross between the durum wheat cultivars Appulo and Adamello. Cappelli is late flowering with vernalization requirement and tall cultivar released in Italy in 1915 derived from the North-African landrace 'Jean Retifah'. The two parents of the mapping population were also used in this study.

2.2. Experimental treatments and phenotypic data used for parameter estimation

A pot experiment with a set of three treatments (LDV, long days vernalized; LDNV, long days nonvernalized; and SDV, short days vernalized) was conducted at Ottava, Sardinia, Italy (41° N 8° E; 225 m above sea level; Giunta et al., 2018; Sanna et al., 2014) to estimate the genetic parameters of the model. Seeds of similar size were imbibed for 24 h at room temperature on water saturated Whatman paper discs in Petri dishes. For the nonvernalized treatment, germinated seeds were directly transplanted in 5 L pots (three seeds per pot) filled with 1:2 (v:v) mixture of sand and sandy-clay-loam soil. For the two vernalized treatments, germinated seeds were transferred in a controlled-temperature cabinet where they were maintained for 40 days at 4°C in the dark. At the end of the vernalization treatments their coleoptile was about 3-cm long and the first seminal root was about 4-cm long. The two long day treatments were potted on 24 May and the short-day vernalized treatment was potted on 23 December of the same year. Two pots were used for each RIL/treatment combination and were arranged in a completely randomized design. The May-sown plants were maintained outdoors, and the December-sown ones were kept in a greenhouse. The pots were watered and fertilized as required. Daily weather data were recorded in a meteorological station located 300 m from the field, temperatures were recorded inside the greenhouse near the plants. The environmental conditions for the three treatments are summarized in Supplementary Table S1.

The plants were monitored twice weekly to record the number and length of the leaves which had appeared on the main stem, the appearance of the flag leaf ligule, and anthesis on main stem. Anthesis was recorded when 50 % of the anthers on the ear of the main stem were visible (that is, Zadoks growth stage 65; Zadoks et al., 1974). The Haun stage (decimal leaf stage) was calculated following Haun (1973):

$$LS = n + \frac{l}{L} \quad (1)$$

where n is the number of ligulated leaves, l is the exposed length of leaf n+1 at the time of measurement, and L is the final length of the blade of leaf n+1. The exposed length of a leaf was measured with a ruler as the distance from leaf tip to the upper collar of the sheath tube.

2.3. Description of the wheat phenology model

We used a modified version of the wheat phenology model described by He et al. (2012) integrated in the crop growth model SiriusQuality (Martre and Dambreville, 2018; Martre et al., 2006). The model is based on the framework proposed by Jamieson et al. (1998). It considers that vegetative and reproductive development is not independent and is coordinated and overlap in time (Hay and Kirby, 1991; Kirby, 1990). The successive appearance of leaves on the main-stem and tillers is the expression of the vegetative development, while anthesis is a particular stage in the reproductive development of the plant. Within this framework, the variations associated with vernalization requirement and daylength (DL) sensitivity are described in terms of primordium initiation, leaf production, and final main stem leaf number.

The leaf production phase is modeled based on two independently controlled processes, leaf initiation (primordia formation) and emergence (leaf tip appearance). The interaction between these processes leads to the determination of the final number of leaves (L_f) produced on the main stem. At any time during vegetative development the number of apex primordia (PN) is calculated through a metric relationship with

leaf number under the assumption that the apex contains four primordia at plant emergence (PN_{ini}) and that they accumulate at twice the rate of leaf emergence (PNslope; Brooking and Jamieson, 2002):

$$PN = PN_{slope} \times L + PN_{ini} \quad (2)$$

temperature (T_{min}^{ver}) to a maximum for an optimum temperature (T_{opt}^{ver}). For temperature above T_{opt}^{ver}, under short days, V_{rate} reduces to zero at the maximum vernalizing temperature (T_{max}^{ver}), while under long days, V_{rate} stays at its maximum value. The effectiveness of short days decreases progressively as photoperiods increases. V_{rate} is given by:

$$V_{rate} = \begin{cases} 0, & T_{apex} < T_{min}^{ver} \\ VAI \times T_{apex} + VBEE, & T_{min}^{ver} \le T_{apex} \le T_{opt}^{ver} \\ \max\left(0, \left(VAI \times T_{opt}^{ver} + VBEE\right) \times \left(1 + \frac{T_{opt}^{ver} - T_{apex}}{T_{max}^{ver} - T_{opt}^{ver}} \times \frac{\max(DL_{min}, \min(DL_{sat}, DL)) - DL_{min}}{DL_{sat} - DL_{min}}\right)\right), & T_{opt}^{ver} < T_{apex} < T_{max}^{ver} \end{cases} \quad (5)$$

The rate of leaf appearance is described with a segmented linear model (Jamieson et al., 1995a) where the first three leaves appear more rapidly than the next ones:

$$L = \begin{cases} P_{decr} \times \frac{T_t}{P_{SD}}, & L < L_{decr} \\ \frac{T_t}{P_{SD}}, & L \ge L_{decr} \end{cases} \quad (3)$$

where L is the number of appeared leaves on the main stem (equivalent to the Haun stage), T_t is the thermal time accumulated by the apex since plant emergence; P_{SD} is the phyllochron modified by sowing date for the first three leaves; P_{decr} is a factor (set at 0.75) decreasing the phyllochron for leaf number less than L_{decr}; and L_{decr} is the Haun stage (set at 3 leaves) up to which the phyllochron is decreased by P_{decr}. Thermal time since plant emergence (T_t) is calculated using a linear model of daily mean temperature with a base temperature of 0°C. Initially the controlling temperature (apex temperature) is assumed to be that of the near soil surface (0–2 cm), and then that of the canopy after Haun stage 4. Near soil surface temperature and canopy temperature are calculated using a surface energy balance model (Jamieson et al., 1995b).

Many studies have shown that phyllochron depends on the sowing date (e.g. Baumont et al., 2019; McMaster et al., 2003; Slafer and Rawson, 1997). In *SiriusQuality*, for a winter sowing (day of the year 1–90 for the Northern hemisphere) the phyllochron decreases linearly with the sowing date and is minimum until mid-July for the Northern hemisphere (day of the year 200; He et al., 2012):

$$P_{SD} = \begin{cases} P \times \left(1 - R_P \times \min\left(SD, SD_{W/S}\right)\right), & 1 \le SD < SD_{S/A} \\ P, & SD \ge SD_{S/A} \end{cases} \quad (4)$$

where SD is the sowing date in day of the year; P is the phyllochron for autumn sowing; R_P is the rate of decrease of P_{SD} for winter sowing; $SD_{W/S}$ and $SD_{S/A}$ are the sowing dates for which P_{SD} is minimum and maximum, respectively.

Vernalization progress and photoperiodic responses are modeled as sequential processes. Vernalization starts once the seed has imbibed water, which is assumed to take one day. In winter wheat, and other cereals, vernalization requirement can be eliminated or greatly reduced by a prolonged exposure to short DL (Dubcovsky et al., 2006; Evans, 1987), a process referred as short day vernalization. We modified the vernalization model described by He et al. (2012) to account for this process. The photoperiodic effect on the vernalization rate is likely to involve a quantitative interaction with temperature rather than a complete replacement of the vernalization requirement (Allard et al., 2012; Brooking and Jamieson, 2002). In the revised model, the daily vernalization rate (V_{rate}) increases at a constant rate (VAI) with daily mean temperature from its value (VBEE) at the minimum vernalizing

where $T_{apex}$is the apex temperature, DL is the day length of the current day, and DL_{sat} and DL_{min} are the saturation and minimum DL for short day vernalization, respectively. The progress toward full vernalization (V_{prog}) is simulated as a time integral:

$$V_{prog} = \min\left(1, \sum_{day=1}^{n} V_{rate}\right) \quad (6)$$

Two parameters define the minimum (L_{min}^{abs}) and maximum (L_{max}^{abs}) number of leaves that can be initiated on the main stem. The model assumes that plants start with a high potential leaf number (L_{pot} set to an initial value of L_{max}^{abs}) which decreases with vernalization progress:

$$L_{pot} = L_{max}^{abs} - \left(L_{max}^{abs} - L_{min}^{abs}\right) \times V_{prog} \quad (7)$$

Vernalization is complete when one of the following three conditions is met: (1) V_{prog} equals 1; (2) L_{pot} equalsL_{min}^{abs}; or (3) L_{pot} equals PN. All the primordium formed during the vernalization phase are assumed to produce leaves. L_{max}^{abs} corresponds to the number of leaves produced by a winter genotype grown under long days at a temperature above T_{max}^{ver}.

The plant responds to DL only once vernalization is completed. DL sensitivity leads to an increase in the number of leaf primordia resulting from the vernalization routine. If DL of the day when vernalization is completed exceeds a given value (DL_{sat}), the final leaf number on main stem (L_f) is set to the value calculated at the end of the vernalization routine and the floral initiation stage is reached. For DL shorter than DL_{sat}, Brooking et al. (1995) have shown that L_f is determined by DL at the stage of two leaves after the flag leaf primordium has been formed. This creates the need for an iterative calculation of an approximate final leaf number (L_{app}) that stops when the required leaf stage is reached:

$$L_{app} = \max\left(L_{pot}, L_{pot} + SLDL \times \left(DL_{sat} - DL\right)\right) \quad (8)$$

where, SLDL is a parameter defining the day length response as a linear function of DL. It is assumed that the attainment of the stage "two leaves after flag leaf primordium" is reached when half of the leaves have emerged (Brooking et al., 1995):

$$0.5 \times L_{app} \le L, \text{ then } L_f = L_{app} \quad (9)$$

When this condition is fulfilled, transition to floral initiation is completed and L_f is equal to the number of primordia formed on that day. Anthesis occurs a fixed number of phyllochron (PFLLAnth) after the appearance of the flag ligule.

The model described above has been developed as an independent executable component (Manceau and Martre, 2018) in the BioMA software framework (Donatelli and Rizzoli, 2008) integrated in the wheat model *SiriusQuality*, version 2.0.57777 (He et al., 2012; Martre and Dambreville, 2018; Martre et al., 2006).

Table 1
Name, symbol, definition, nominal, minimal, and maximal value, unit and calibration criteria of the calibrated genetic parameters of *SiriusQuality* phenology sub-model. The four parameters were optimized sequentially in order they are shown in the table.

Name	Definition	Value			Unit	Calibration criteria	Method	Treatment used for calibration[a]
		Nominal	Min	Max				
L_{min}^{abs}	Minimum absolute main stem leaf number	-	7.8	11.3	Leaf	Final leaf number	Measured	LDV
P	Phyllochron	110	80	140	°Cd leaf^{-1}	Haun stage	Estimated	LDV
PFLLAnth	Phyllochronic duration of the period between flag leaf ligule appearance and anthesis	2.4	1.5	3.5	-	Anthesis date	Estimated	LDV
SLDL	Daylength response of leaf production	0.7	0	2.5	leaf h^{-1} (DL)	Flag leaf ligule appearance date	Estimated	SDV
VAI	Response of vernalization rate to temperature	0.001	0	0.015	d^{-1}°Cd^{-1}	Flag leaf ligule appearance date	Estimated	LDNV

[a] LDV, long day vernalized; SDV, short day vernalized; LDNV, long day non vernalized.

2.4. Estimation of the ecophysiological model parameters

Five parameters of the phenology model were estimated for each of the 91 RILs using the three treatments of the pot experiment described above (Table 1). These parameters were estimated based a previous study which showed that *P*, SLDL and VAI are enough to predict genetic variability of winter wheat genotypes (He et al., 2012; Rincent et al., 2017). PFLLAnth and L_{min}^{abs} were also estimated because a previous analysis of the data set used for parameter estimation in this study revealed a significant genetic variability for these two traits (Sanna et al., 2014).

We designed a calibration procedure that minimizes the interactions between the different components of phenology. First, three parameters controlling earliness *per se* (*P*, L_{min}^{abs},PFLLAnth) were estimated with the LDV treatment. L_{min}^{abs} was set equal to the measured value of L_f, then *P* and PFLLAnth were estimated sequentially by minimalizing the root mean squared error (RMSE) for Haun stage and the absolute error (AE) for anthesis date, respectively. Then the sensitivity to DL (SLDL) was estimated by minimizing the AE for the date of flag ligule appearance for SDV treatment. Finally, the slope of the response vernalization rate to temperature (VAI) was estimated by minimizing the AE for the date of flag ligule appearance for LDV treatment. Parameters were estimated with the Brent hybrid root-finding algorithm (Brent, 1973) by using the 'optim' function of the 'stats' package of the R software program, version 4.1.3 (R Core Team, 2022). The other parameters of the model were set to the values given by He et al. (2012), except L_{decr}, T_{pot}^{ver} and T_{max}^{ver} which were increased following the work of Brown et al. (2013) and VBEE that was also increased following Robertson et al. (1996) to take into account the lower response of vernalization rate to temperature for durum wheat compared with winter bread wheat(Supplementary Table S2). All simulations started on the sowing date.

2.5. Genetic map and quantitative trait loci detection

An updated version of the Ofanto × Cappelli genetic map previously reported (Marone et al., 2012) was developed and used for QTL analysis of the parameter values. Whole-genome profiling was performed using the DArT-Seq™ technology (Diversity Arrays Technology Pty Ltd, Australia). DArT-Seq™ detects both single nucleotide polymorphisms (SNPs) and presence–absence sequence variants, collectively referred to as DArT-Seq™ markers. Briefly, the genetic map is composed of 32 linkage groups which cover all of the chromosomes except 1 A. The total number of markers is 9267, of which 4033 on the A genome and 5594 on the B genome. The number of markers per chromosome ranges from 162 (4B) to 1217 (6B). The map length spanned 2119.2 cM, with 965.5 cM for the A genome, and 1153.7 cM for the B genome.

QTL analysis was performed using the Composite Interval Mapping method (Zeng, 1994) with the Qgene software, version 4.3.10 (Joehanes and Nelson, 2008). Scanning interval of 1 cM between markers and tentative QTL with a window size of 10 cM was used to detect QTL. Marker cofactors for background control were set by single marker regression and simple interval analysis with a maximum of five controlling markers. Major QTL were defined as two or more linked markers associated with a parameter with a logarithm of odds (LOD) score > 5.0 and a phenotypic variance contribution > 10 %. QTL with a LOD score > 2.8 and a phenotypic variance contribution < 10 % were defined as moderate QTL. Tentative QTL with a LOD score between 1.0 and 2.8 were also considered for the prediction of QTL-based parameters. For main QTL effects, the positive sign of the estimates indicates that Ofanto allele contributed to the higher values of the parameter. The intervals of the QTL and flanking markers were determined following the method described by Darvasi and Soller (1997). The proportion of phenotypic variance explained by a single QTL was determined by the square of the partial correlation coefficient (r^2). Graphical representation of linkage groups was carried out using the MapChart software, version 2.2 (Voorrips, 2002).

The available sequences of DArT-seq markers (provided by Triticarte, www.diversityarrays.com) were used as queries in a BLAST against the 'Svevo' genome (Maccaferri et al., 2019) to assign a physical interval to QTL identified in the present study. Similarly, available sequences of known genes involved in flowering time control in wheat and other species were used as queries in a BLAST search to identify their physical position onto the 'Svevo' genome. Physical position on the 'Svevo' genome of common markers mapped in previously published studies was also used for comparison with known QTL for phenological traits in tetraploid wheat.

2.6. Quantitative trait loci prediction of the phenology model parameters

QTL-based values for each of the five estimated parameters were estimated for each RIL considering only additive QTL actions. Our aim was to be built a predictive model, therefore, all QTL with LOD score > 1 were considered. Following the approach used by Bogard et al. (2014), linear models for the five calibrated ecophysiological parameters were obtained using multiple linear regressions with backward elimination of the QTL by fitting the following statistical model to the estimated parameters values:

$$\widehat{y}_j = \widehat{m} + \sum_{i=1}^{n} \widehat{a}_i \times g_{ij} \quad (10)$$

where $\widehat{m}$ is the estimated intercept, $\widehat{a}_i$ is the estimated additive effect of the *i*-th QTL on the phenology model parameter, and $g_{i,j}$is the allele of the *j*-th RIL at the *i*-th QTL. The Ofanto alleles were coded +1 and those of Cappelli −1.

2.7. Field experiment for original and QTL-based model validation

Estimated and QTL-based values of the five parameters were used to simulate the development of the 91 RILs grown in the field during the 2012–2013 growing seasons at Ottava (experiment names OT13) and during the 2007–2008 (FO08) and 2008–2009 (FO09) growing seasons

at Foggia, Italy (41.46° N, 15.55° E, 76 m a.s.l.). In Foggia, each line was planted at a rate of 40 seeds per row (1-m long) with 0.3-m interrow spacing. In Ottava, the RILs were sown with a 6-row planter at a density of 350 seeds m^{-2}. Each plot consisted of six rows with an interrow spacing of 0.18 m and had a surface area of 10 m^2. At both sites the seeds were sown in a randomized complete block design with three replications. These three experiments were not used for parameter estimation. Anthesis dates was recorded at Ottava for each line and the two parents, while at Foggia heading date was recorded and anthesis date was estimated from the relationship obtained with OT13 data between thermal time to anthesis and thermal time to heading ($r^2 = 0.95$, $P < 0.001$). Haun stage, final leaf number, flag leaf ligule appearance and anthesis dates were also recorded at Ottava using the protocol described above for the pot experiment. For all field experiments arithmetic means of all traits were calculated. Predictions using the QTL-based model parameters were compared with predictions using the estimated (original) parameters.

The QTL-based based model was also evaluated for the two parents, which were not used for QTL analysis, in the three environments described above, and in five (Cappelli) or 15 (Ofanto) other site/year/sowing date combinations. Cappelli was grown during the 2003–2004 growing season at Ottava with late-November and mid-February sowing dates and during the 2004–2005 growing season with early-January and mid-March sowing dates, and at Oristano, Sardinia, Italy (40° N, 8° W, 15 m a.s.l.) with mid-January sowing date. Ofanto was grown for eight consecutive years (harvests 1992–1999) at Ottava with sowing dates between mid-November and early-January, and at Oristano for seven years (harvests 1993–2000) with sowing dates between late-November and early-February. In all experiment, crops were sown at a density of 350 viable seeds m^{-2}. Each plot was 7-m long with 8-rows and an interrow spacing of 0.18 m. The experimental design was a randomized complete block design with three replicates. The sowing dates and summary environmental conditions for all the trials are given in Supplementary Table S1. All trials were rainfed and other crop inputs including pest, weed and disease control, and nitrogen, potassium, and phosphate fertilizers were applied at levels to prevent nutrients or pests, weeds, and diseases from limiting plant development and growth. All crops were simulated from the day of sowing. At each site, daily weather data were recorded from meteorological stations located in the experimental farms near the experimental fields. For each parent, parameters values were obtained from the corresponding model linking genetic markers to model parameters and the model was used to predict the anthesis date.

2.8. Statistics for model evaluation

Several statistics were calculated to assess the quality of the model simulation results. The observed and simulated data were compared using ordinary least square regression and the mean squared error (MSE). To get a better understanding of the model errors, the MSE was decomposed in non-unity slope (NU), squared bias (SB) and lack of correlation (LC) following Gauch et al. (2003). Spearman's rank correlation coefficient (ρ) was also calculated. All data analysis and graphs were done using R statistical software program version 4.2 (R Core Team, 2022).

3. Results

3.1. Estimations of the genetic parameters of the phenology model

The five estimated parameters showed large genetic variability between the RILs and significant transgressive segregation (Fig. 1). Ofanto and Cappelli had close values for *P* and SLDL. VAI was the most different parameter between the parents, with Cappelli having a much lower value than Ofanto. VAI had a clear bimodal distribution and the two parents had values close to the two peaks of the distribution. PFLLAnth was significantly correlated with *P* and SLDL ($r = 0.40$ and -0.27, respectively). The strongest correlation between parameters was between L_{min}^{abs} and SLDL ($r = -0.66$), although L_{min}^{abs} was measured in the LDV treatment and SLDL was estimated with the SDV treatments.

3.2. Quantitative trait loci analysis and QTL-based prediction of model parameters

The genetic analysis of the estimated parameter values identified 13 moderate and major QTL (Table 2). All these QTL colocalized with known QTL for wheat phenology (Table 2). The percentage of variance of the parameters explained by each QTL varied between 14 % (QTL 3 for *P*) and 44 % (QTL 15 for VAI). No major or moderate QTL was identified for PFFLAnth but several tentative QTL colocalized with known QTL, including a QTL (QTL29, LOD = 2.0) previously identify for DL sensitivity of heading date for winter wheat (Table 2). Two (for VAI) to five (for L_{min}^{abs}) moderate or major QTL were identified for each of the other four parameters. Only one of these, QTL28, was associated with two model parameters (SLDL and L_{min}^{abs}), the other moderate and major QTL were associated with only one model parameter, but QTL2 (for L_{min}^{abs}) and QTL27 (for *P*) included a tentative region for SLDL (Fig. 3).

Two moderate QTL (LOD > 2.8) for L_{min}^{abs} colocalized with known developmental genes (Fig. 3); QTL30 colocalized with Vrn-B3, and QTL32 with Vrn-A2 and FT-A5. *Vrn-A2* was also close to QTL16 for SLDL but not within the QTL confidence interval. We also found one tentative QTL for L_{min}^{abs} (and SLDL), QTL5, that colocalized with Ppd-B1 loci. For VAI, the major QTL15 colocalized with Vrn-A1 on chromosome 5 A, and the peak marker for two tentative QTL, QTL1 and QTL8, colocalized with CO-B9 and FT-A2, respectively. The peak marker of QTL23 for *P* colocalized with CO-B2 locus. For the other two parameters, PFLLAnth and SLDL, the only associations to known developmental genes regarded putative QTLs. For PFLLAnth, QTL25 colocalized with Co-A1 locus and for SLDL, the peak marker of QTL2 and QTL5 colocalized with ELF-B1 and Ppd-B1 loci, respectively.

The five genetic parameters of *SiriusQuality* were estimated using the 79 QTL with a LOD score > 1. Eleven significant QTL and 21 tentative QTL with a LOD score value between 1 and 2.8 were used as predictors in the fitted statistical models (Table 2). *P*, SLDL, VAI, PFLLAnth and, L_{min}^{abs} were predicted with 11, 10, 8, 6, and 10 QTL, respectively. QTL 32, which collocated at *Vrn-A2* was not selected in the multilinear model to predict L_{min}^{abs}, but the tentative QTL16, close to *Vrn-A2,* was used to predict SLDL. Seven tentative QTL collocated with several parameters. Tentative QTL8 and QTL14 were associated with four of the five parameters, the other five tentative QTL (QTL1, QTL5, QTL7, QTL10, and QTL25) were associated with two parameters.

The coefficients of the multi-linear model (Table 2) were well correlated with the additive effect of the QTL (all $r^2 > 0.87$ and $P < 0.002$), except for SLDL ($r^2 = 0.01$, P = 0.56). Thirty one of the 33 tentative QTL used to predict the parameters colocated with known QTL for heading date or other wheat phenology traits (Table 2). The fitted multi-linear model predicted the five parameters without significant bias (Fig. 3), they explained 36 % (for PFLLAnth) to 63 % (for *P* and L_{min}^{abs}) of the genotypic variation of the parameters. The relative RMSE for *P*, SLDL, VAI, PFLLAnth and, L_{min}^{abs} were 1.7 %, 18.9 %, 30.7 %,9.6 %, and 4.1 %, respectively. The QTL-based parameters of the two parents of the RILs were also well estimated, especially for Cappelli (Fig. 3).

3.3. Predictions of leaf stage

As illustrated in Fig. 4 for the lines with the highest (135.9 leaf °Cd^{-1}) and lowest (118.6 leaf °Cd^{-1}) values of *P*, the model parametrized with the estimated (original) parameters predicted well the rate of main stem leaf appearance for the treatment LDV used to estimated *P* (Fig. 2A) but also for the treatments not used to estimate it (SDV, LDNV;

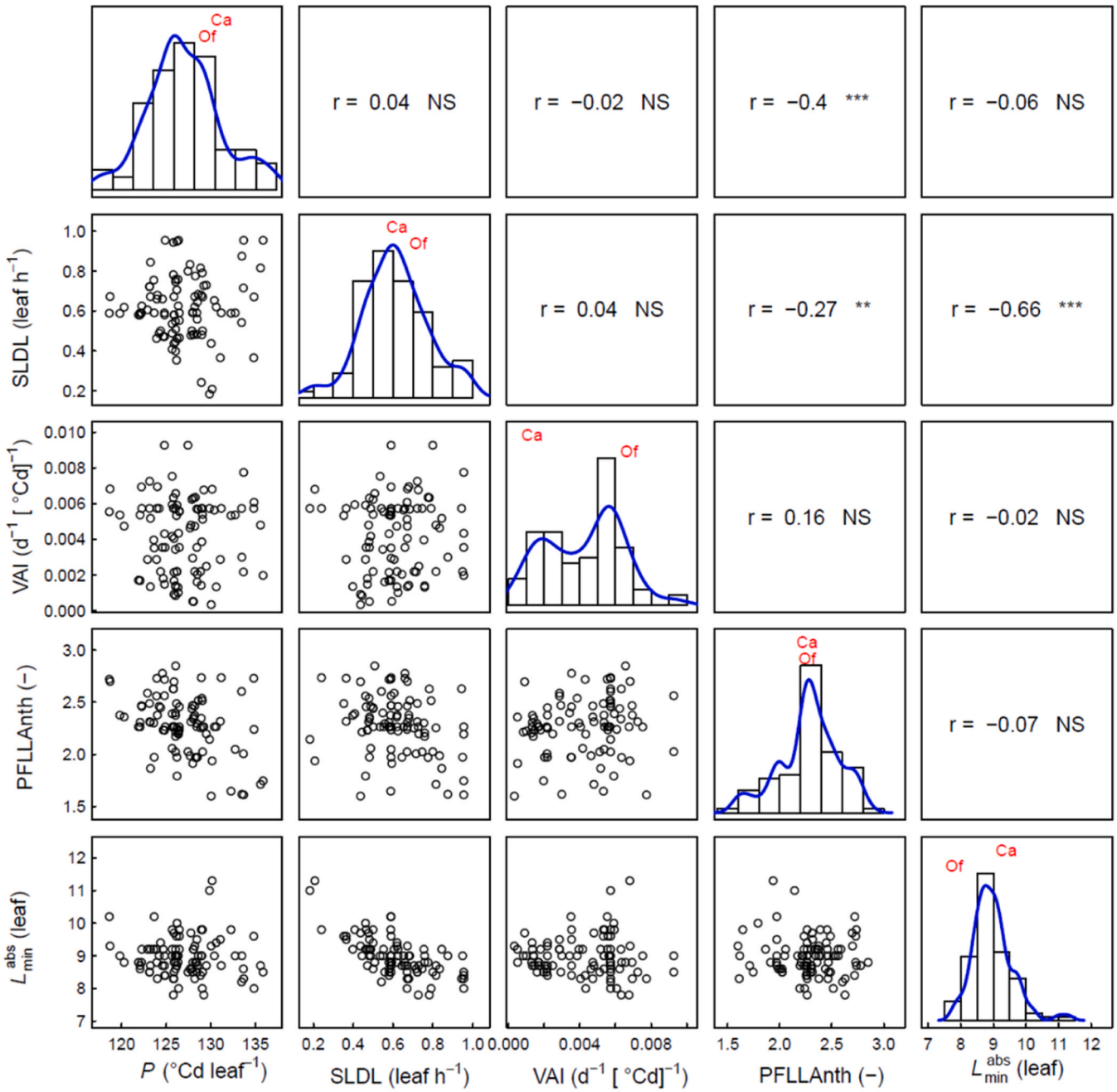

Fig. 1. Distribution and correlations between the genetic parameters of *SiriusQuality* phenology model for 91 RILs of the Ofanto (Of) × Cappelli (Ca) cross. The phyllochron (*P*), the sensitivity to day length (SLDL), the response of the vernalization rate to temperature (VAI), and the number of phyllochron between flag leaf ligule appearance and anthesis (PFLLAnth) were estimated sequentially each using one of the three environments of the calibration dataset, while L_{min}^{abs} was measured in the LDV treatment. Correlation coefficients are reported above the diagonal. NS, not significant; **, $P < 0.01$; ***, $P < 0.001$.

Fig. 2C,E), as well as for the field experiment OT13 (Fig. 2G). For the latter experiment, the RMSE for main stem leaf number was only 0.15 leaves (Table 2). The QTL-based model also predicted well the rate of leaf appearance in all treatments (Fig. 2C, D, F, and H), and the RMSE for the validation experiment was close to that of the model with the original parameters (Table 2).

3.4. Predictions of final leaf number

The treatments in the calibration experiment had large effects on L_f. As expected, on average L_f was the lowest for LDV (averaging 9.0 leaves) and the highest for LDNV (averaging 13.6 leaves; Fig. 3A). The genetic variability of L_f was also much higher for the LDNV-grown plants than for the two other treatments. The model explained 90 % of the genotypic variation of L_f for the mean of the three treatments (Table 2) but only 35 % for SDV. For the field experiment of the validation data set where L_f was recorded (OT13), the RMSE was only 0.46 leaves, but the model explained 20 % of the genotypic variance. The RMSE for L_f was about two-times higher for the QTL-based model than for the model with the estimated parameters. The higher error of the QTL-based model was mainly due to a higher lack of correlation (Table 2). However, for validation data set both models gave similar results.

Table 2

QTL used to predict the five genetic parameters of *SiriusQuality* phenology model. Two moderate QTL (QTL 31 and 32) not used to predict SLDL and L_{min}^{abs} are also indicated in italic face. *P*, phyllochron; SLDL, daylength (DL) sensitivity; VAI, rresponse of vernalization rate to temperature; L_{min}^{abs}, absolute final leaf number; PFLLAnth, Phyllochronic duration of the period between flag leaf ligule appearance and anthesis. Major (LOD < 5 and $r^2 > 0.1$) and moderate (LOD > 2.8) QTL are indicated in bold face.

Parameter	QTL no.	Chromosome-linkage group	Position (cM)	Confidence interval (cM)	Peak marker	Flanking markers	Physical interval (Mb)	Peak LOD value	r^2[a]	Additive effect[b]	Coefficient of multilinear model	Colocation with QTL	Phenotyped traits	Environments[d]
P	**23**	**6BL**	**69**	**7.8**	**5325371**	**2258129–1236305**	**545.7–594.4**	**5.2**	**0.24**	**1.439**	**1.20837**	QTL 47 in Giunta et al. (2018)	Spikelets spike^{-1}	Field
	27	**7BL**	**8**	**8.1**	**1112963**	**5567157–1402975**	**468.1 – 537.0**	**4.9**	**0.23**	**−1.543**	**−1.25825**	QTL A.30 in Le Gouis et al. (2012)	Heading (°Cd)	Field (3 years) and different combinations of DL and vernalization in the greenhouse
												QTL 54 in Giunta et al. (2018)	Phyllochron	Pots outdoor, long-day
												Mengistu et al. (2016)	Booting (d), anthesis (d), maturity (d)	Field (2 years x 2 sites)
												Giraldo et al. (2016)	Heading (d)	Field (4 year / site combinations)
	3	**2BS**	**6**	**13.5**	**1862383**	**1080014–5411598**	**0.4 – 8.9**	**2.8**	**0.14**	**−1.015**	**−0.77854**	Sukumaran et al. (2018)	Anthesis (d), maturity (d)	Field (potential, drought, and high temperature)
												Q.ICD.Ppd−05 Gupta et al. (2020)	Heading (°Cd)	Weak vs strong vernalization
	25	7 AS	0	15.1	1128723	1128723–5353667	165.3 – 281.8	2.5	0.12	−0.962	−0.97753	QTL 50 in Giunta et al. (2018)	Final Leaf number	Pots greenhouse, vernalized
													Anthesis (°Cd), fruiting efficiency	Field
	10	3BL	147	17.8	4004851	2276928–1130481	750.1 – 774.6	2.1	0.10	−0.894	−0.97620	QTL 6 in Sanna et al. (2014)	Final leaf number, terminal spikelet to anthesis (°Cd)	Pots greenhouse, vernalized
												QTL 22 in Giunta et al. (2018)	Final Leaf number	Pots greenhouse, vernalized
												Q.ICD.Eps−07 in Gupta et al. (2020)	Heading (°Cd)	13 field experiments at different latitudes
												Soriano et al. (2017)	Booting (d), anthesis(d), maturity (d)	3 years x 2 sites in Spain
												Maccaferri et al. (2014)	Heading (d)	27 field trials (years x sites at different latitudes)
	6	2BL	2	19.3	2249524	5325236–3961379	617.0 – 698.9	1.9	0.10	1.218	0.56940	QTL 13 in Giunta et al. (2018)	Flag leaf appearance (°Cd), anthesis (°Cd)	Pots greenhouse, vernalized
												Soriano et al. (2017)	Booting (d), anthesis (d), maturity (d)	3 years x 2 sites in Spain

(*continued on next page*)

Table 2 (*continued*)

Parameter	QTL no.	Chromosome-linkage group	Position (cM)	Confidence interval (cM)	Peak marker	Flanking markers	Physical interval (Mb)	Peak LOD value	r^2[a]	Additive effect[b]	Coefficient of multilinear model	Colocation with QTL	Phenotyped traits	Environments[d]
												Giraldo et al. (2016)	Heading (d)	Field (4 year / site combinations)
	24	7A	20	22.1	2279140	1009498–1011692	703.4–722.6	1.7	0.08	−1.022	−0.40842	QTL0165 in Giraldo et al. (2016)	Heading (d)	Field (4 year / site combinations)
												QTL0829 in Mengistu et al. (2016)	Booting (d), anthesis (d), maturity (d)	Field (2 years x 2 sites)
	17	5 A	18	23.8	4405595	4542293–5367049	2.5 – 11.4	1.5	0.08	0.816	0.70204	QTL 11 in Sanna et al. (2014)	Leaves number at terminal spikelet, anthesis (°Cd)	Pots outdoor, long-day
												QTL 36 in Giunta et al. (2018)	Anthesis (°Cd)	Pots greenhouse, vernalized
												Q.ICD.Vrn−24 in Gupta et al. (2020)	Heading (°Cd)	13 field experiments at different latitudes
												Roncallo et al. (2017)	Heading (d), anthesis (d)	6 field trials in Argentina, sowing from July to August
	19	6AL	83	24.4	2261280	4394087–5563094	582.8 – 598.7	1.5	0.07	0.723	0.36715	QTL 43 in Giunta et al. (2018)	Phyllochron, fruiting efficiency	Pots outdoor, long-day
												Soriano et al. (2017)	Booting (d), anthesis (d), maturity (d)	3 years x 2 sites
												Giraldo et al. (2016)	Heading (d)	Field (4 year / site combinations)
	8	3AL	15	25.8	1088186	5580236–1089657	28.1 – 219.6	1.4	0.08	−0.739	−0.63557	QTL 16 in Giunta et al. (2018)	Flag leaf appearance (°Cd)	Field
													Final leaf number	Pots outdoor, long-day vernalized
													Flag leaf appearance (d) and anthesis (d)	Pots outdoor, long-day
												Sukumaran et al. (2018)	Anthesis (d), maturity (d)	Field (potential, drought, and high temperature)
												Maccaferri et al. (2011)	Heading (d)	15 field trials
												Maccaferri et al. (2014)	Heading (d)	27 field trials (years x sites at different latitudes)
	14	4AL	54	31.0	2253908	1205880–4410019	24.2 – 137.3	1.2	0.06	0.673	0.68804	QTL 26 in Giunta et al. (2018)	Leaf number at terminal spikelet, ear fertility	Pots outdoor, long-day
												Q.ICD.Eps−22 in Gupta et al. (2020)	Heading (°Cd)	Weak vs strong vernalization
												Maccaferri et al. (2011)	Heading (d)	15 field trials
												Milner et al. (2016)	Heading (d), maturity (d)	4 field trials at three locations

(*continued on next page*)

Table 2 (*continued*)

Parameter	QTL no.	Chromosome-linkage group	Position (cM)	Confidence interval (cM)	Peak marker	Flanking markers	Physical interval (Mb)	Peak LOD value	r^2[a]	Additive effect[b]	Coefficient of multilinear model	Colocation with QTL	Phenotyped traits	Environments[d]
SLDL	**9**	**3AL**	**52**	**10.6**	**Xgwm1042**	**W01T03c - 2295584**	**561.3 – 591.8**	**3.6**	**0.17**	**−0.06**	**−0.02775**	Meta-QTL in Griffiths et al. (2009)	Heading (d)	23 field trials at 5 sites
												Maccaferri et al. (2014)	Heading (d)	27 field trials (years x sites at different latitudes)
	28	**7BL**	**86**	**10.8**	**3021883**	**5582872–1121517**	**680.7 – 687.3**	**3.6**	**0.17**	**−0.018**	**0.05714**	QTL 14 in Sanna et al. (2014)	Final leaf number, leaf number at terminal spikelet	Pots outdoor, long-day vernalized
													Penultimate leaf to anthesis (°Cd)	Pots outdoor, long-day
												QTL 55 in Giunta et al. (2018)	Final leaf number, maximum tiller number	Pots outdoor, long-day vernalized
													Spikelet spike^{-1}	Pots outdoor, long-day
													Spikelet spike^{-1}	Pots greenhouse, vernalized
												Q.ICD.Eps−32 in Gupta et al. (2020)	Heading (°Cd)	Weak vs strong vernalization
												Roncallo et al. (2017)	Heading (d), anthesis (d)	6 field trials in Argentina, sowing from July to August
	31	***2 AL***	***30***	***12.5***	***980420***	***4398088–3946769***	***735.3 – 754.4***	***3.0***	***0.15***	***−0.053***	***NA***[c]	QTL 7 in Giunta et al. (2018)	Fruiting efficiency	Pots outdoor, long-day vernalized
													Anthesis (°Cd)	Pots greenhouse, vernalized
												Q.ICD. Ppd−04)in Gupta et al. (2020)	Heading (°Cd)	Weak vs strong vernalization
	27	7BL	18	15.8	1018944	992708–4993835	518.1 – 583.8	2.4	0.12	0.045	0.03314	QTL A.30 in Le Gouis et al. (2012)	Heading (°Cd)	Field (3 years) + different combinations of DL and vernalization in the greenhouse
												QTL 54 in Giunta et al. (2018)	Flag leaf appearance (°Cd), anthesis (°Cd)	Pots outdoor, long-day vernalized
												Mengistu et al. (2016)	Booting (d), anthesis (d), maturity (d	Four field trials (Etiopia)
	10	3BL	141	22.1	1089762	4003283–1130262	731.3 – 770.3	1.7	0.08	0.047	0.01998	QTL 6 in Sanna et al. (2014)	Leaf number at TS, duration various pre-anthesis phenophases (°Cd)	Pots greenhouse, vernalized

(*continued on next page*)

Table 2 (*continued*)

Parameter	QTL no.	Chromosome-linkage group	Position (cM)	Confidence interval (cM)	Peak marker	Flanking markers	Physical interval (Mb)	Peak LOD value	r^2[a]	Additive effect[b]	Coefficient of multilinear model	Colocation with QTL	Phenotyped traits	Environments[d]
												QTL 22 in Giunta et al. (2018)	Final leaf number	Pots greenhouse, vernalized
												Q.ICD.Eps−07 in Gupta et al. (2020)	Heading (°Cd)	13 field experiments at different latitudes
												Soriano et al. (2017)	Booting (d), anthesis (d), maturity (d)	3 years x 2 sites
												Maccaferri et al. (2014)	Heading (d)	27 field trials (years x sites at different latitudes)
	2	1BL	12	26.9	4535838	1231191–1101118	652.9 – 678.5	1.4	0.07	0.042	0.02962	QTL 4 in Giunta et al. (2018)	Final leaf number	Pots outdoor long-day vernalized,
	7	2BL	68	28.2	1109533	3064932–4409889	757.0 – 762.5	1.3	0.07	−0.033	−0.02670	QTL 15 in Giunta et al. (2018)	Phyllochron	Pots outdoor long-day vernalized, pots greenhouse vernalized
												QTL 2B.3 in Ruan et al. (2020)	Anthesis (d)	3 years at one location
												Soriano et al. (2017)	Booting, anthesis and maturity (d)	3 years x 2 sites in Spain
	14	4AL	68	28.6	4410019	2253908–4009690	426.7 – 577.3	1.3	0.06	0.043	0.03965	QTL 26 in Giunta et al. (2018)	Leaf number at terminal spikelet, grains spike^{-1}	Pots outdoor, long-day
												Q.ICD.Eps−22 in Gupta et al. (2020)	Heading (°Cd)	Weak vs strong vernalization
												Maccaferri et al. (2011)	Heading (d)	15 field trials
												Milner et al. (2016)	Heading (d), maturity (d)	4 field trials at three locations
	5	2BS	2	32.7	3934592	wPt−5788–1020393	55.8 – 69.6	1.1	0.06	−0.039	−0.03767	QTL 4 in Sanna et al. (2014)	Anthesis (°Cd)and different pre-anthesis phenophases (°Cd)	Pots greenhouse, vernalized
												QTL 1 in Panio et al. (2013)	Heading (d), leaf porosity	Field, 2 years at one location
												QHd.ubo−2B in Milner et al. (2016)	Heading (d), maturity (d)	4 field trials at three locations
												QTL 11 in Giunta et al. (2018)	Flag leaf appearance (°Cd), anthesis (°Cd)	Pots greenhouse, vernalized
												Q.ICD.Ppd−05 in Gupta et al. (2020)	Heading (°Cd)	Weak vs strong vernalization
												Marcotuli et al. (2017)	Heading (d)	Field trials (2 sites, 1 year)
												Soriano et al. (2017)	Booting (d), anthesis (d), maturity (d)	Field trials (3 years x 2 sites) in Spain

(*continued on next page*)

Table 2 (*continued*)

Parameter	QTL no.	Chromosome-linkage group	Position (cM)	Confidence interval (cM)	Peak marker	Flanking markers	Physical interval (Mb)	Peak LOD value	r^2[a]	Additive effect[b]	Coefficient of multilinear model	Colocation with QTL	Phenotyped traits	Environments[d]
	4	2BS	48	32.7	1121477	1669700 - Xwmc257	24.9 – 30.2	1.1	0.06	−0.032	−0.03968	QTL 9 in Giunta et al. (2018)	Anthesis (°Cd), flag leaf appearance (°Cd)	Pots greenhouse, vernalized
													Anthesis (°Cd)	Field
												QTL 2B.1 in Ruan et al. (2020)	Anthesis (d)	Field (potential, drought, and high temperature)
												Maccaferri et al. (2014)	Heading (d)	27 field trials (years x sites at different latitudes)
	16	5AL	82	33.3	1200768	1088962–2303083	612.4 – 647.0	1.1	0.06	0.038	0.02976	QTL 34 in Giunta et al. (2018)	Spike weight at anthesis	Pots outdoor, long-day
												Q.ICD.Vrn−25 in Gupta et al. (2020)	Heading (°Cd)	Different DL and levels of vernalization
												qHde3 in Nishimura et al. (2018)	Heading (d)	Field (4 years at one site)
												Maccaferri et al. (2014)	Heading (d)	27 field trials (years x sites at different latitudes)
												Roncallo et al. (2017)	Heading (d), anthesis (d)	6 field trials in Argentina, sowing from July to August
												Buerstmayr et al. (2012)	Anthesis (d)	Field, four environments
VAI	**15**	**5AL**	**24**	**4.2**	**5567501**	**3064395–1090215**	**539.6 – 554.2**	**11.1**	**0.44**	**0.00123**	**0.00108**	QTL 10 in Sanna et al. (2014)	Phyllochron, anthesis (°Cd), leaf number at terminal spikelet, final leaf number	Pots outdoor, long-day
												Meta-QTL M18 in Griffiths et al. (2009)	Heading (d)	23 field trials (five sites)
												QTL 33 in Giunta et al. (2018)	Leaf number at terminal spikelet, final leaf number, anthesis (°Cd), maximum tiller number	Pots outdoor, long-day
												Q.ICD.Vrn−11 in Gupta et al. (2020)	Heading (°Cd)	Different DL and levels of vernalization
	21	**6BL**	**41**	**12.6**	**3029892**	**3947529–3029892**	**23.9 – 26.5**	**3.0**	**0.15**	**0.00100**	**0.00045**	QTL0612 in Maccaferri et al. (2011)	Heading (d)	15 field trials
												QTL0655 in Maccaferri et al. (2014)	Heading (d)	27 field trials (years x site at different latitudes)
	8	3AL	28	15.4	1089657	1166451–1237528	103.2 – 481.9	2.4	0.12	−0.00050	−0.00040	QTL 16 in Giunta et al. (2018)	Final leaf number	Pots outdoor, long-day vernalized

(*continued on next page*)

Table 2 (*continued*)

Parameter	QTL no.	Chromosome-linkage group	Position (cM)	Confidence interval (cM)	Peak marker	Flanking markers	Physical interval (Mb)	Peak LOD value	r^2[a]	Additive effect[b]	Coefficient of multilinear model	Colocation with QTL	Phenotyped traits	Environments[d]
													Flag leaf appearance (°Cd), anthesis (°Cd)	Pots outdoor, long-day
												Sukumaran et al. (2018)	Anthesis (d), maturity (d)	Field (potential, drought, and high temperature)
												Maccaferri et al. (2011)	Heading (d)	15 field trials
												Maccaferri et al. (2014)	Heading (d)	27 field trials (years x site at different latitudes)
	12	4AL	23	20.6	4008720	4541315–5579508	609.2 – 628.9	1.8	0.09	0.00067	0.00024	QTL 24 in Giunta et al. (2018)	Leaf number o at terminal spikelet	Pots outdoor, long-day vernalized
													Final leaf number, flag leaf appearance (°Cd), anthesis (°Cd)	Pots outdoor, long-day
													Final leaf number	Field
												Maccaferri et al. (2011)	Heading (d)	15 field trials
	18	5BC	60	22.3	5323929	1271726 - Gpw4463	396.1 – 428.4	1.7	0.08	0.00061	0.00049	QTL A.23 in Le Gouis et al. (2012)	Heading (°Cd)	Field (3 years) and different combinations of DL and vernalization the greenhouse
												QTL 38 in Giunta et al. (2018)		
	Phyllochron	Pots greenhouse, vernalized												
												Q.ICD.Vrn−12 in Gupta et al. (2020)	heading (°Cd)	Weak vs strong vernalization
	1	1BL	32	22.6	1245938	1042145–4008436	331.4 – 493.6	1.6	0.08	0.00061	0.00033	QTL 1 in Sanna et al. (2014)	Terminal spikelet (°Cd)	Pots outdoor, long-day
												Hd_Cad12 in Milner et al. (2016)	Heading (d), maturity (d)	4 field trials at 3 sites
												QTL 1 in Giunta et al. (2018)	Phyllochron	Field
												Milner et al. (2016)	Heading (d), maturity (d)	4 field trials at three sites
												Soriano et al. (2017)	Booting (d), anthesis (d), maturity (d)	3 years x 2 sites
												Maccaferri et al. (2011)	Heading (d)	15 field trials
												Maccaferri et al. (2014)	Heading (d)	27 field trials (years x sites at different latitudes)

(*continued on next page*)

Table 2 (*continued*)

Parameter	QTL no.	Chromosome-linkage group	Position (cM)	Confidence interval (cM)	Peak marker	Flanking markers	Physical interval (Mb)	Peak LOD value	r^2[a]	Additive effect[b]	Coefficient of multilinear model	Colocation with QTL	Phenotyped traits	Environments[d]
	22	6BL	14	23.8	3935283	3570667–1055879	670.1 – 689.7	1.6	0.08	−0.00059	−0.00025	QTL 45 in Giunta et al. (2018)	Leaf number at the end of tillering	Pots greenhouse, vernalized
												Q.ICD.Vrn−15 in Gupta et al. (2020)	Heading (°Cd)	Across 4 'phenological environments'
												Giraldo et al. (2016)	Heading (d)	Field (4 year / site combinations)
PFLLAnth	29	7BL	9	18.5	1264692	Mag600–1252669	695.7 – 705.2	2.0	0.10	0.094	0.05277	QTL A.31 in Le Gouis et al. (2012)	Heading (°Cd)	Field (3 years) and different combinations of DL and vernalization in the greenhouse
												QTL 57 in Giunta et al. (2018)	Final leaf number	Pots outdoor, long-day vernalized
													Flag leaf appearance (°Cd), anthesis (°Cd)	Pots greenhouse, vernalized
												Maccaferri et al. (2011)	Heading (d)	15 field trials
												Maccaferri et al. (2014)	Heading (d)	27 field trials (years x sites at different latitudes)
												Roncallo et al. (2017)	Heading (d), anthesis (d)	6 field trials in Argentina, sowing from July to August
	20	6AL	114	22.9	1043765	1090518–1699304	602.0 – 609.2	1.6	0.08	−0.083	−0.07448	QTL 44 in Giunta et al. (2018)	grains spike^{-1}	Pots greenhouse, vernalized
												Maccaferri et al. (2011)	Heading (d)	15 field trials
	13	4AL	0	23.8	1076004	1076004–1068548	3.3 – 4.6	1.6	0.08	−0.085	−0.08634			
	25	7AS	4	25.1	1019140	1128723–1270127	165.3 – 516.5	1.5	0.07	−0.077	−0.06582	QTL 50 in Giunta et al. (2018)	Final leaf number	Pots greenhouse, vernalized
													Phyllochron, fruiting efficiency, flag leaf appearance (°Cd), anthesis (°Cd)	Field
	8	3AL	15	31.0	1088186	1370441–1089657	21.7 – 117.8	1.2	0.06	0.071	0.05761	QTL 16 in Giunta et al. (2018)	Flag leaf appearance (°Cd), anthesis (°Cd)	Pots outdoor, long-day
												Sukumaran et al. (2018)	Anthesis (d), maturity	Field (potential, drought, and high temperature)
												Maccaferri et al. (2011)	Heading (d)	15 field trials
												Maccaferri et al. (2014)	Heading (d)	27 field trials (years x sites at different latitudes)

(*continued on next page*)

Table 2 (*continued*)

Parameter	QTL no.	Chromosome-linkage group	Position (cM)	Confidence interval (cM)	Peak marker	Flanking markers	Physical interval (Mb)	Peak LOD value	r^2[a]	Additive effect[b]	Coefficient of multilinear model	Colocation with QTL	Phenotyped traits	Environments[d]
	11	3BL	6	35.9	Xgwm181	2267290–5011369	824.5 – 837.9	1.0	0.05	0.061	0.08194	Hd_Pr11 in Milner et al. (2016)	Heading (d), maturity (d)	Four field trials at 3 sites
												QTL 23 in Giunta et al. (2018)	Leaf number at terminal spikelet	Pots greenhouse, vernalized
													Flag leaf appearance (°Cd), anthesis (°Cd)	Field
												Maccaferri et al. (2014)	Heading (d)	27 field trials (years x sites at different latitudes)
L_{min}^{abs}	**28**	**7BL**	**90**	**4.9**	**1113703**	**1092265–1120350**	**685.0 – 689.9**	**9.0**	**0.37**	**−0.338**	**−0.12836**	QTL 14 in Sanna et al. (2014)	Leaf number at terminal spikelet, final leaf number	Pots outdoor, long-day vernalized
													Penultimate leaf to anthesis (°Cd)	Pots outdoor, long-day
												QTL 55 in Giunta et al. (2018)	Flag leaf appearance (°Cd), final leaf number	Pots outdoor, long-day vernalized
													Spikelet spike^{-1}	Pots outdoor, long-day
												Q.ICD.Eps−32 in Gupta et al. (2020)	Heading (°Cd)	Weak vs strong vernalization
												Roncallo et al. (2017)	Heading (d), anthesis (d)	6 field trials in Argentina, sowing from July to August
	2	**1BL**	**62**	**6.2**	**4910793**	**4535838 - Xgwm659**	**661.0 – 672.2**	**6.8**	**0.30**	**−0.251**	**−0.17304**	QTL 4 in Giunta et al. (2018)	Final leaf number	Pots outdoor, long-day vernalized
	30	**7B**	**0**	**9.0**	**1065475**	**1065475–1112171**	**7.6 – 15.5**	**4.4**	**0.20**	**−0.273**	**−0.20360**	QTL 58 in Giunta et al. (2018)	Flag leaf appearance (°Cd), anthesis (°Cd), final leaf number, spikelet spike^{-1}	Pots outdoor, long-day vernalized
													Anthesis (°Cd)	Pots outdoor, long-day
												Q9_FT_19 and Q10_FT_17 in Wright et al. (2020)	Anthesis (d)	Field and pots, spring sowing
	26	**7AL**	**50**	**11.0**	**Xgwm276**	**3064654–1074583**	**627.4 – 639.2**	**3.5**	**0.17**	**0.175**	**0.06228**	Meta-QTL in Griffiths et al. (2009)	Heading (d)	23 field trials (five sites)
												Kuchel et al. (2006)	Heading (d)	Winter and summer sowings, artificial light, vernalization
												QTL 51 in Giunta et al. (2018)	Final leaf number	Pots outdoor, long-day vernalized
													Final leaf number	Pots greenhouse, vernalized

(*continued on next page*)

Table 2 (*continued*)

Parameter	QTL no.	Chromosome-linkage group	Position (cM)	Confidence interval (cM)	Peak marker	Flanking markers	Physical interval (Mb)	Peak LOD value	r^2[a]	Additive effect[b]	Coefficient of multilinear model	Colocation with QTL	Phenotyped traits	Environments[d]
	32	***5AL***	***20***	***11.5***	***2261896***	***978762–4405542***	***639.7 – 662.8***	***3.3***	***0.16***	***−0.249***	***NA***[c]	QTL 35 in Giunta et al. (2018)	Heading (d)	Pots outdoor, long-day vernalized
	18	5BC	60	14.8	5323929	Xbarc74 - Gpw4463	401.5 – 428.4	2.6	0.12	0.146	0.09500	QTL A.23 in Le Gouis et al. (2012)	Heading (°Cd)	Field (3 years) and different combinations of DL and vernalization in the greenhouse
												QTL 38 in Giunta et al. (2018)	Phyllochron	Pots greenhouse, vernalized
												Q.ICD.Vrn−12 in Gupta et al. (2020)	Heading (°Cd)	Weak vs strong vernalization
	8	3AL	21	18.3	4009170	3022183–1089657	61.6–219.6	2.0	0.10	0.195	0.08899	QTL 16 in Giunta et al. (2018)	Final leaf number	Pots outdoor, long-day vernalized
													Flag leaf appearance (°Cd)	Field
												Sukumaran et al. (2018)	Anthesis (d), maturity (d)	Field, 2 years (potential, drought, and high temperature)
												Maccaferri et al. (2011)	Heading (d)	15 field trials
												Maccaferri et al. (2014)	Heading (d)	27 field trials (year x sites at different latitudes)
	1	1BS	18	20.3	1066594	1723461–1688943	113.5 – 386.9	1.8	0.09	0.182	0.13833	QTL 1 in Sanna et al. (2014)	Terminal spikelet (°Cd)	Pots outdoor, long-day
												Hd_Cad12 in Milner et al. (2016)	Heading(d), maturity (d)	4 field trials at 3 sites
												QTL 1 in Giunta et al. (2018)	Phyllochron	Field
												Milner et al. (2016)	Heading (d), maturity (d)	4 field trials at 3 sites
												Soriano et al. (2017)	Booting (d), anthesis (d), maturity (d)	3 years x 2 sites
												Maccaferri et al. (2011)	Heading (d)	15 field trials
												Maccaferri et al. (2014)	Heading date (d)	27 field trials (years x sites at different latitudes)
	7	2BL	64	22.3	3950327	3064932–4409889	757.0 – 762.5	1.7	0.08	−0.174	−0.09350	QTL 15 in Giunta et al. (2018)	Phyllochron	Pots greenhouse, vernalized
												QTL 2B.3 in Nishimura et al. (2018)	Anthesis (d)	Field (potential, drought, and high temperature)

(*continued on next page*)

Table 2 (*continued*)

Parameter	QTL no.	Chromosome-linkage group	Position (cM)	Confidence interval (cM)	Peak marker	Flanking markers	Physical interval (Mb)	Peak LOD value	r^2[a]	Additive effect[b]	Coefficient of multilinear model	Colocation with QTL	Phenotyped traits	Environments[d]
												Soriano et al. (2017)	Booting (d), anthesis (d), maturity (d)	3 years x 2 sites
	5	2BS	12	26.2	3958859	wPt−5788–1004499	55.8–80.7	1.4	0.07	−0.16	−0.09943	QTL 4 in Sanna et al. (2014)	Leaf number at terminal spikelet	Pots outdoor, long-day vernalized
													Anthesis and pre-anthesis phenophases (°Cd)	Pots greenhouse, vernalized
												QTL 1 in Panio et al. (2013)	Heading (d)	Field trials, 2 years
												QHd.ubo−2B in Milner et al. (2016)	Heading (d), maturity (d)	4 field trials at 3 sites
												QTL 11 in Giunta et al. (2018)	Spikelet number	Pots outdoor, long-day
													Flag leaf appearance (°Cd), anthesis (°Cd)	Pots greenhouse, vernalized
												Q.ICD.Ppd−05 in Gupta et al. (2020)	Heading (°Cd)	Different levels of vernalization; short vs normal DL
												Marcotuli et al. (2017)	Heading time	Field, 2 sites, 1 year
												Soriano et al. (2017)	Booting (d), anthesis (d), maturity (d)	Field, 3 years x 2 sites in Spain
	14	4AL	56	28.6	3024608	3948025–4410019	24.2 – 137.3	1.3	0.06	−0.154	−0.06812	QTL 26 in Giunta et al. (2018)	Leaf number at terminal spikelet, grain spike^{-1}	Pots outdoor, long-day
												Q.ICD.Eps−22 in Gupta et al. (2020)	Heading (°Cd)	Weak vs strong vernalization
												Maccaferri et al. (2011)	Heading (d)	15 field trials
												Milner et al. (2016)	Heading (d), maturity (d)	4 field trials at 3 sites

[a] Percent of explained phenotypic variance calculated during the QTL detection using MapQTL.
[b] Additive effect of the Ofanto allele.
[c] QTL not included in the multi-linear model of parameter prediction.
[d] Plants were sow under short-day unless otherwise indicated.

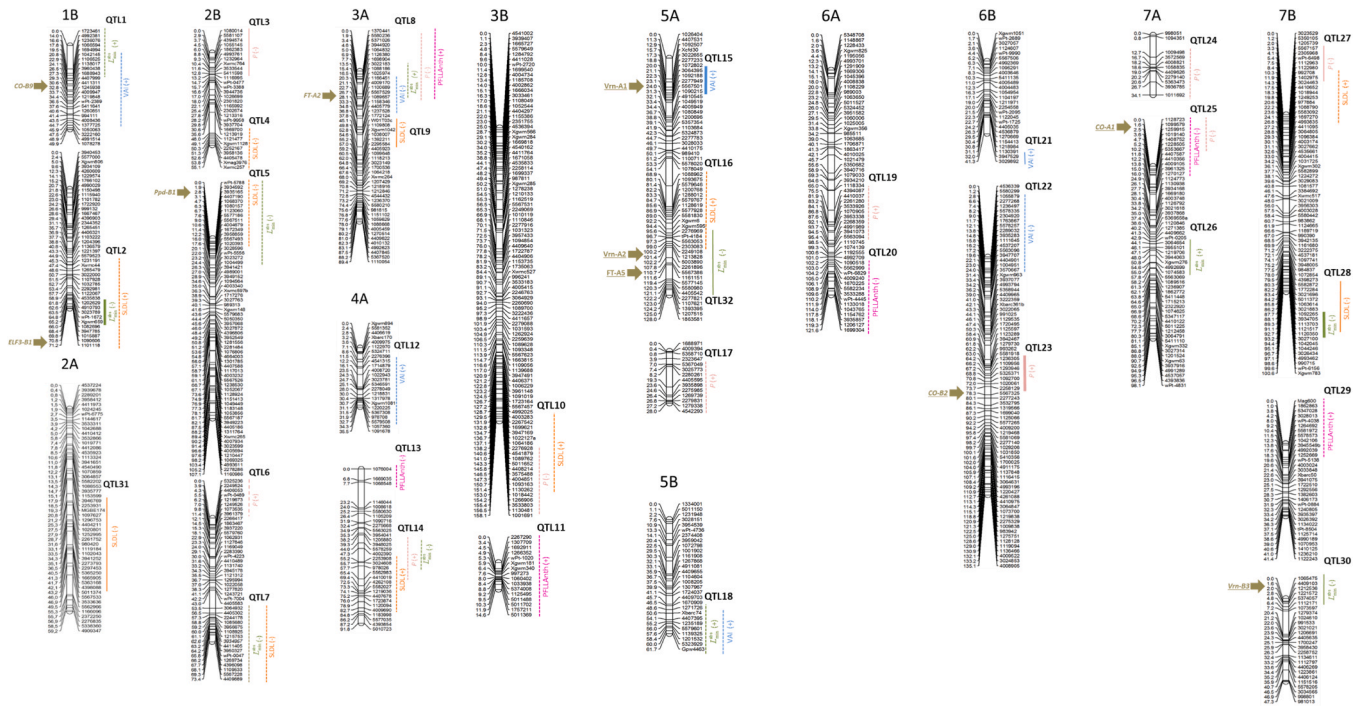

Fig. 2. Chromosomal regions harboring QTL for the five genetic parameters of the *SiriusQuality* phenology model for the Ofanto × Cappelli RILs population. Genetic distances (cM) are indicated on the left of each linkage group, marker codes are indicated on the right. The vertical bars indicate the 95 % confidence intervals (CI). Dashed CI bars indicate tentative QTL with $1 < LOD < 2.8$; solid CI bars indicate moderate QTL with $2.8 \leq LOD < 4.9$; thick solid CI bars indicate major QTL with $LOD \geq 5$. Signs in parenthesis after the parameter names indicate the sign of the additive effect of the Offanto allele. Major phenology genes in segregation in the population are indicated by horizontal arrows on the left of the linkage groups.

3.5. Predictions of flag leaf ligule appearance date

In the calibration experiment, the average number of days between seed imbibition and the appearance of the flag leaf ligules was 56, 73, and 135 for the LDV, SDV, and LDNV, respectively (Fig. 3B). The shorter duration for LDV compared with LDNV was due to the low temperature during the vernalization treatment. The lower number of leaves for LDV compared to LDNV did not compensate for the low rate of leaf emergence during the vernalization treatment for LDV. The model predicted the flag leaf ligule appearance date with a RMSE of 0.9 days for the mean of the three treatments used for parameter estimation (Fig. 3C, Table 2) and explained 60 % (for LDV) to 99 % (for SDV) of the genotypic variance. The RMSE was more than three-folds higher for LDNV and LDV than for SDV. For the validation trial for which the flag leaf ligule appearance was recorded (OT13), the RMSE was significantly higher (4 days) than for the calibration data set. The model explained only 28 % of the genotypic variance for flag leaf ligule appearance date for OT13 (Table 2, Fig. 4C), which was mainly responsible for the model error (LC accounted for 70 % of the MSE).

For LDV, the RMSE for the days to flag leaf ligule appearance were similar for the QTL-based model and the model with the estimated parameters, while for the LDNV and SDV it was about two- and five-times higher for the QTL-based model than for the model with the estimated parameters. For the validation data (OT13), the RMSE of both models were similar, but the QTL-based model explained only 11 % of the genetic variation of the date of flag leaf ligule appearance, compared with 65 % for the model with the estimated parameters. The ranking of the lines was better conserved ($\rho = 0.58$ and 0.36 with the original and QTL-based parameters, respectively). Fig. 5

3.6. Predictions of anthesis date

In the calibration experiment, the number of days to anthesis was about two-times higher for SDV than for the long day treatments (Fig. 3E). The genotypic variability was also much higher for SDV-grown plants. Although three of the five genetic parameters were estimated with the LDV treatment, the model explained less of the genotypic variance for this treatment than for the other two (Table 3). Across the three treatments of the calibration experiment, the RMSE for anthesis date ranged from 1.7 (SDV) to 3.9 (LDNV) days and the r^2 ranged from 0.46 (LDV) to 0.89 (SDV). In the three independent field experiment, the RMSE and r^2 for the mean anthesis across the RILs were 2.0 days and 0.56, respectively. In OT13 and FO08, the model error was mainly due to a lack of correlation, while in FO09 about half was due to a lack of correlation and non-unity slope.

For the validation data set, the RMSE for anthesis date was 0.2–0.8 days higher for the QTL-based model compared with the model with the estimated parameters (Table 3, Fig. 6F). On average over the three experiments of the validation data set, the QTL-based model explained 34 % of the genetic variation of anthesis date, which is slightly more than half of the genetic variation explained by the model with the estimated parameters. The ranking of the lines was more conserved between the estimated and QTL-based parameters (0.76 vs. 0.59).

3.7. Predictions of anthesis date for untested genotypes in untested environments

The QTL-based model was further evaluated for the two parents of the RIL population grown in the field in experiments not used for parameter estimation. The two parents were not used to identify QTL, it is thus a test of the ability of the QTL-based model to predict untested genotypes. Across all site/year/sowing date combinations, the number of days to anthesis ranged from 71 to 170 days for Cappelli and from 94 to 171 days for Ofanto. The model with the original parameters predicted anthesis date for Cappelli and Ofanto with a RMSE of 6.2 and 7.3 days and a r^2 of 0.98 and 0.85, respectively (Table 3, Fig. 7A). The RMSE of the QTL-based was higher than that of the original model by 2.4 days

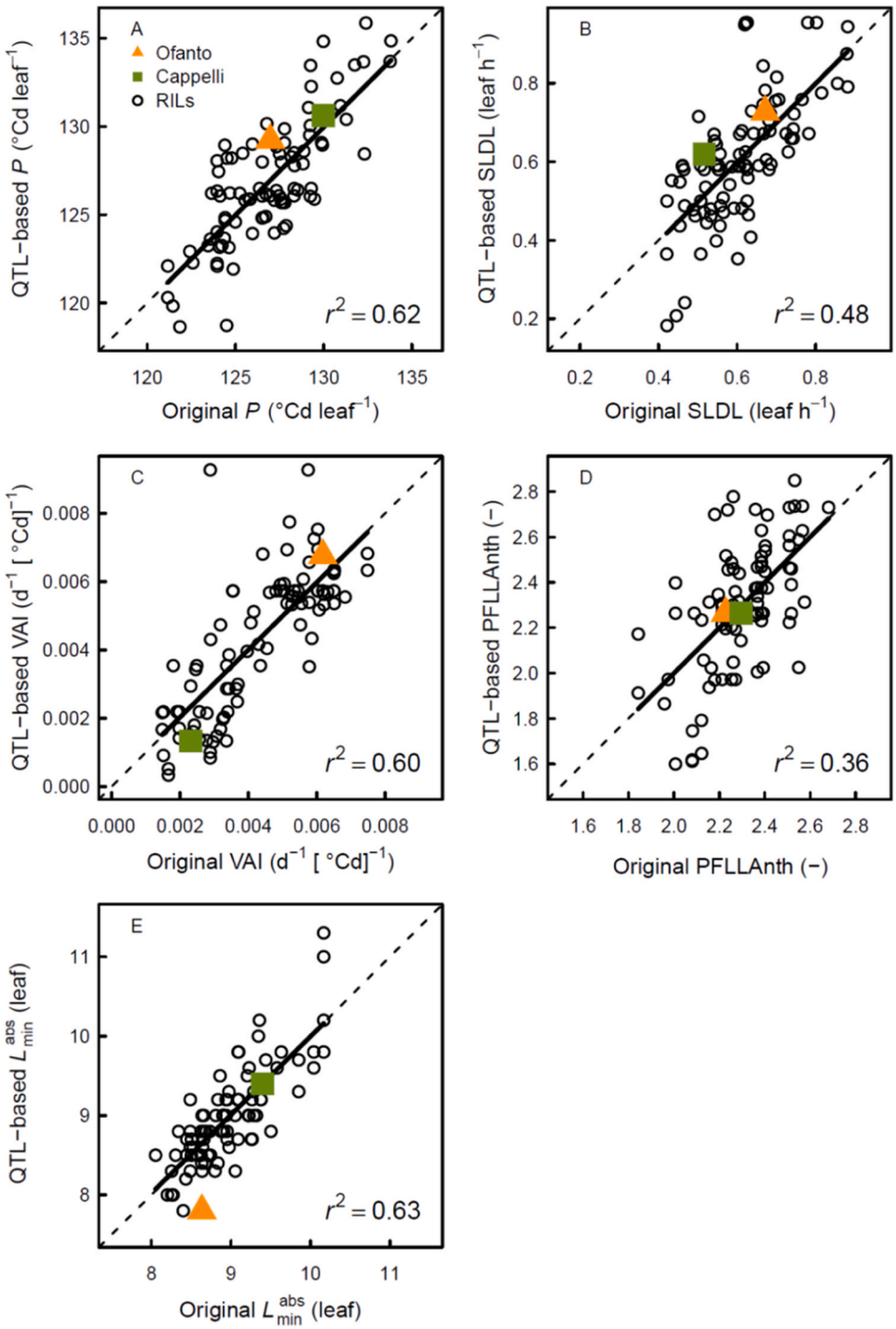

Fig. 3. QTL-based versus original estimations of the five genetic parameters of the *SiriusQuality* phenology model for 91 RILs of the Ofanto (Of) × Cappelli (Ca) cross. The phyllochron (*P*), the sensitivity to day length (SLDL), the response of the vernalization rate to temperature (VAI), and the number of phyllochron between flag leaf ligule appearance and anthesis (PFLLAnth) were calibrated using the three environments of the calibration dataset, while the absolute minimum leaf number (L_{min}^{abs}) was measured in the LDV treatment. Dashed lines are 1:1 lines and solid lines are linear regressions. Note that the two parents were not used for QTL identification.

for Cappelli and was similar for both models for Ofanto (Table 3, Fig. 7B). For Cappelli, the model with both the original and QTL-based parameters had a larger RMSE for the autumn sowing dates (late November – mid December) than for the spring sowing dates (late January – late March). For the QTL based model, the RMSE and r^2 were 7.7 d and 0.97 for the autumn sowing dates and were 9.9 days and 0.59 for the spring sowing dates, respectively.

4. Discussion

Gene- or QTL-based models are useful to integrate ecophysiological, genetic and molecular knowledge and to improve simulation models. They are also powerful tools to predict genotype performance (Chenu et al., 2009), identify ideotypes (Bogard et al., 2020b) or combinations of alleles or loci (Bogard et al., 2020a; Zheng et al., 2016) to adapt genotypes to target environments under current or future climate

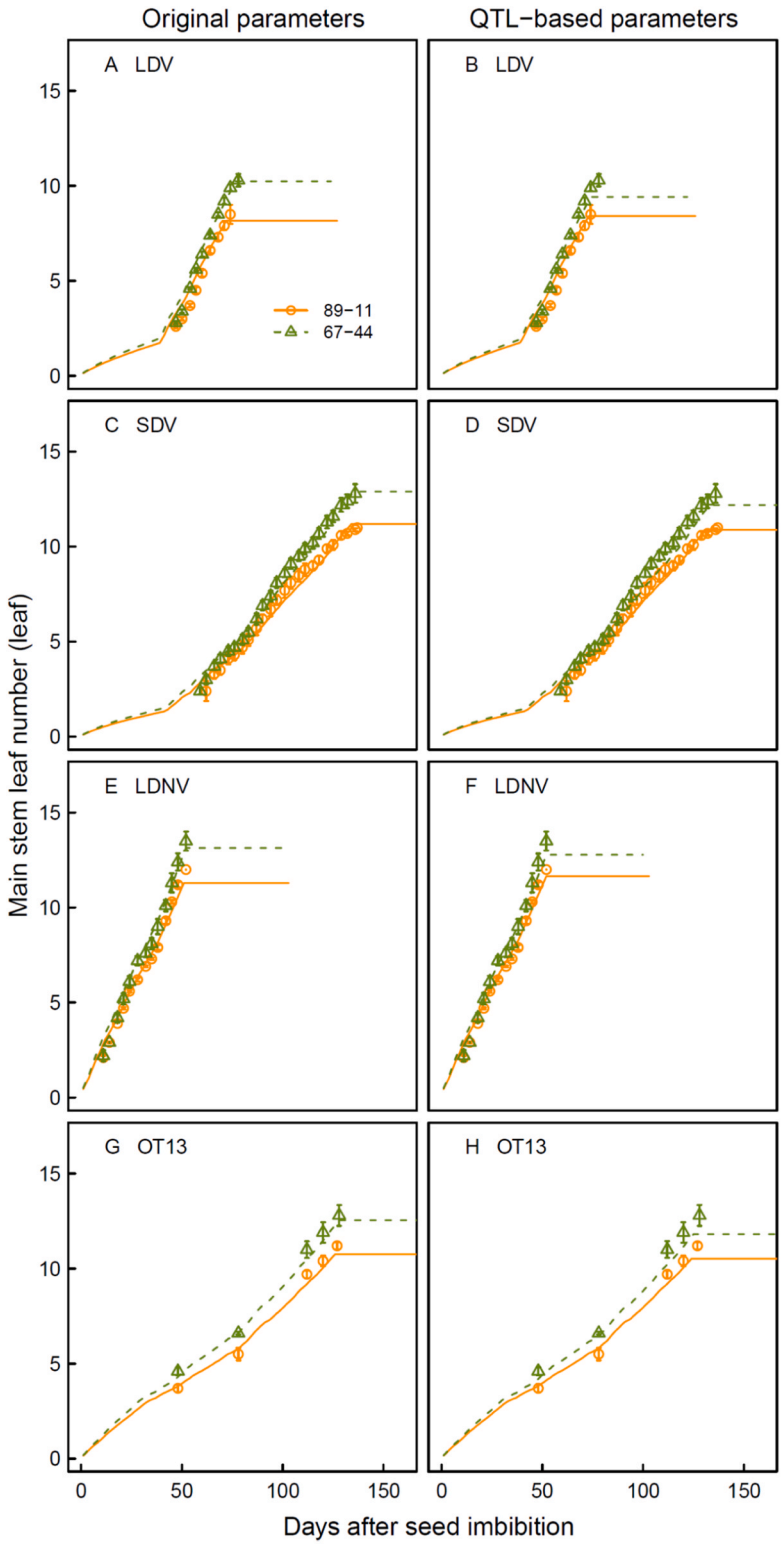

Fig. 4. Haun stage versus days after see imbibition for the two RILs of the Ofanto × Cappelli cross with the highest (89−11) and lowest (67−44) phyllochron for the calibration (A-F) and the validation (G-H) data sets. Symbols are measurements, lines are simulations. The names of the experiments as defined in Table 1 are given in the figure. Simulations were performed with the wheat model *SiriusQuality* using the original (A, C, E, and G) and QTL-based (B,D, F, and H) genetic parameters. Measurements are the mean ± 1 s.d. for $n = 4$ independent replicates.

scenarios, or to design new crop management strategies for specific existing or virtual (new combinations alleles or loci associated with model parameters) genotypes (Martre et al., 2014). In this study, we used a model that integrates our current understanding of the physiology of wheat development and phenology to predict the development and phenology of a RILs population of durum wheat with parameters estimated with vernalization and photoperiod treatments. We identified major or moderate QTL associated with four of the five genotypic parameters of the model. We then used this genetic information to estimate the value of parameters and to predict plant development and anthesis

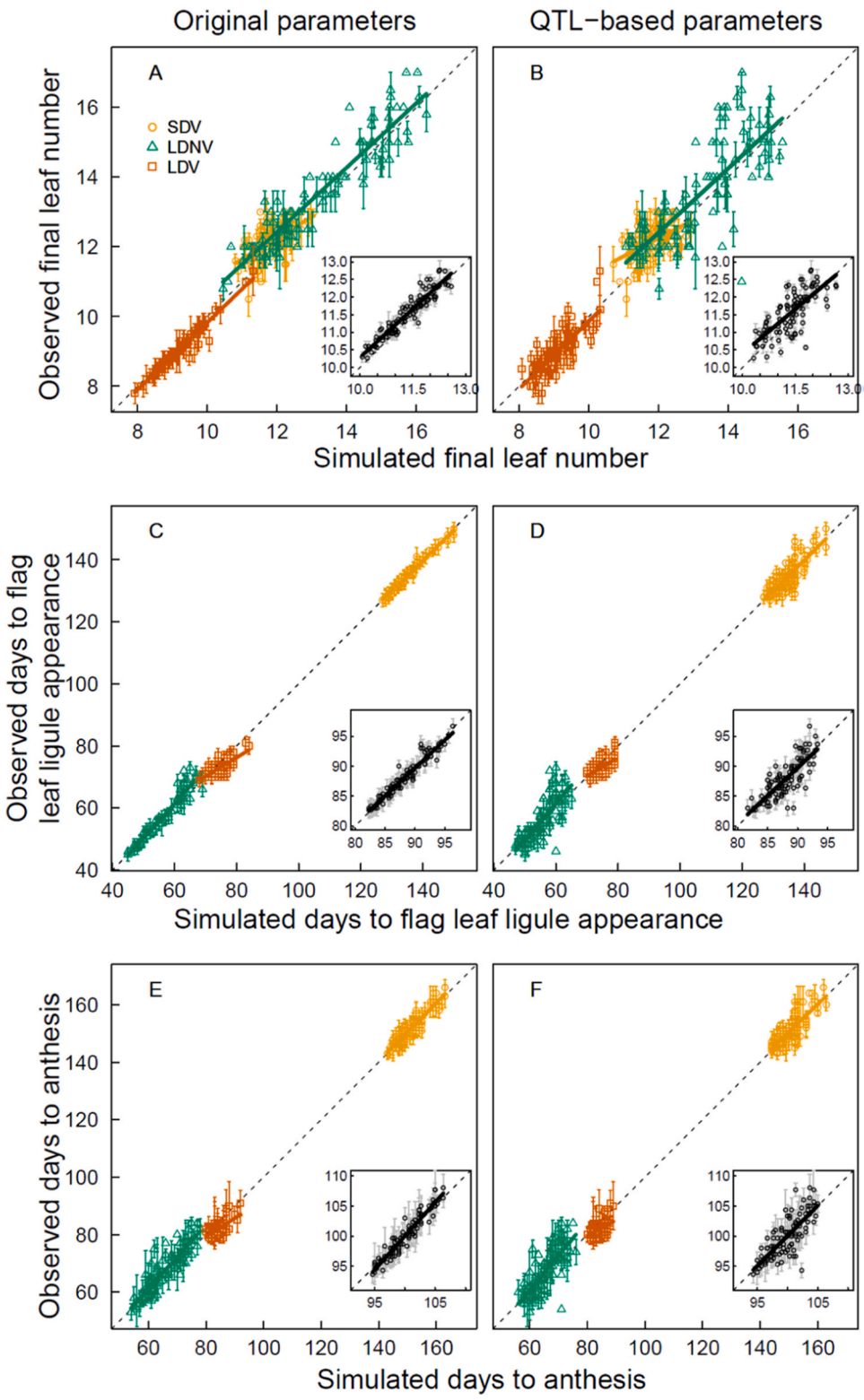

Fig. 5. Observed versus simulated final leaf number (A and B), days to flag leaf ligule appearance (C and D) and days to anthesis (E and F) for 91 RILs of the Ofanto × Cappelli cross. Data are for the short days vernalized (SDV, circles), long days non vernalized (LDN, triangles), and long days vernalized (LDV,squares) treatments of the experiment used to estimate the genetic parameters of the *SiriusQuality* wheat phenology model. Simulations were performed using original (A, C, and E) and QTL-based (B, D, and F) genetic parameters. Inset panels show the mean values for the three experimental treatments. Days to flag leaf ligule and anthesis were calculated from the day after seed imbibition. Dashed lines are 1:1 lines, solid lines are linear regression. Measurements are the mean ± 1 s.d. for $n = 4$ independent replicates.

Table 3
Statistics of model performance to predict days to flag leaf ligule appearance, final leaf number and days to anthesis using the original and the QTL-based parameters for the calibration and the validation data sets. Days to flag leaf ligule and anthesis were calculated from the day after seed imbibition and sowing for the calibration data set and validation data sets, respectively.

Trait	Environment or genotype	Original parameters								QTL-based parameters							
		RMSE[a] (days or leaf)	MSE[a] decomposition (% of MSE)			Linear regression statistics			ρ[a]	RMSE[a] (days or leaf)	MSE[a] decomposition (% of MSE)			Linear regression statistics			ρ[a]
			LC[a]	NU[a]	SB[a]	Slope (-)	Intercept (days or leaf)	r^2			LC[a]	NU[a]	SB[a]	Slope (-)	Intercept (days or leaf)	r^2	
Main stem leaf number	**Calibration data set**																
	Within an experiment																
	LDV	0.54	27	48	25	1.19	−1.47	0.99	0.99	0.54	28	49	23	1.20	−1.53	0.98	0.99
	SDV	0.64	59	13	28	1.08	−0.28	0.97	0.99	0.68	61	12	28	1.09	−0.27	0.97	0.99
	LDNV	0.60	77	9	14	1.05	−0.64	0.98	0.99	0.66	79	11	10	1.07	−0.75	0.97	0.99
	Validation data set																
	OT13	0.15	86	8	6	0.89	0.88	0.85	0.90	0.21	79	16	5	0.78	1.66	0.72	0.82
Final leaf number	**Calibration data set**																
	Within an experiment																
	LDV	0.19	42	1	57	0.97	0.18	0.96	0.98	0.39	91	0	9	0.97	0.13	0.62	0.77
	SDV	0.55	53	12	35	0.60	5.00	0.35	0.58	0.60	54	14	32	0.52	6.02	0.23	0.46
	LDNV	0.65	70	3	27	0.93	1.33	0.88	0.93	1.03	90	1	9	0.92	1.33	0.58	0.76
	Across-RIL mean of environments	0.27	54	4	42	0.92	1.07	0.90	0.95	0.46	81	4	15	0.84	2.01	0.54	0.74
	Validation data set																
	OT13	0.46	64	34	2	0.41	6.92	0.20	0.39	0.49	63	30	7	0.32	7.92	0.10	0.29
Days to flag leaf ligule appearance	**Calibration data set**																
	Within an experiment																
	LDV	2.2	38	25	37	0.60	28.1	0.60	0.70	2.31	55	17	28	0.60	28.52	0.40	0.61
	SDV	0.6	92	4	4	0.98	3.0	0.99	1.00	2.99	100	0	0	0.99	1.83	0.68	0.79
	LDNV	2.1	70	13	17	1.13	−6.1	0.93	0.98	4.41	94	3	4	1.15	−7.68	0.62	0.82
	Across-RIL mean of environments	0.9	88	7	5	0.93	5.8	0.93	0.97	1.98	98	1	1	0.93	5.90	0.63	0.79
	Validation data set																
	OT13	4.0	70	30	0	0.49	65.0	0.28	0.58	4.24	76	21	3	0.40	76.51	0.11	0.36
Days to anthesis	**Calibration data set**																
	Within an experiment																
	LDV	2.9	35	8	57	0.65	26. 9	0.46	0.60	3.1	42	9	49	0.55	35.3	0.25	0.46
	SDV	1.7	93	1	6	1.03	−3.6	0.89	0.93	3.1	97	0	3	0.96	6.3	0.64	0.80
	LDNV	3.9	76	3	21	1.12	−5.9	0.81	0.90	5.3	85	3	12	1.20	−11.4	0.59	0.78
	Across-RIL mean of environments	1.2	89	11	0	1.14	−13.5	0.90	0.96	2.3	100	0	0	1.02	−1.8	0.57	0.76
	Validation data set																
	Within an experiment																
	OT13	1.7	66	28	6	0.69	44.8	0.67	0.82	2.5	62	38	1	0.48	75.2	0.35	0.59
	FO08	3.2	65	29	6	0.46	89.5	0.24	0.50	3.4	61	32	7	0.39	101.6	0.17	0.44
	FO09	2. 6	93	2	5	0.86	21.2	0.41	0.66	3.0	87	6	6	0.69	48.1	0.27	0.53
	Across-RIL mean of environments	2.00	74	17	9	0.70	46.4	0.56	0.76	2.5	67	29	4	0.52	75.1	0.34	0.59
	Cappelli	6.2	62	4	34	0.96	8.4	0.98	0.99	8.6	32	8	61	0.93	15.5	0.98	0.99
	Ofanto	7.3	70	19	11	0.82	28.1	0.85	0.87	7.1	78	21	1	0.82	27.3	0.84	0.86

[a] RMSE, root mean squared error; MSE, mean squared error; LC, lack of correlation; NU, non-unity slope; SB, squared biased; ρ, Spearman's correlation coefficient.

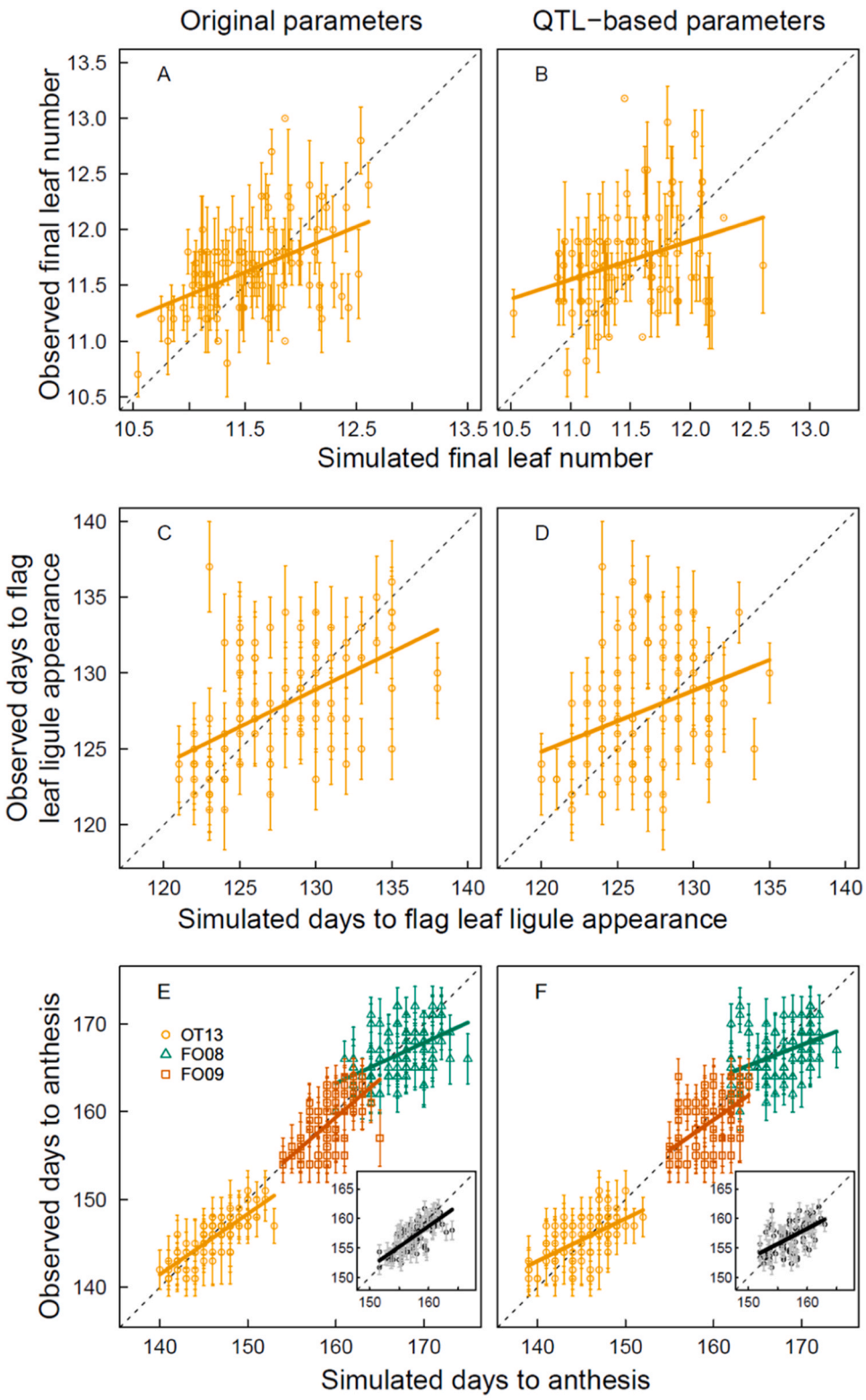

Fig. 6. Observed versus simulated final leaf number (A and B), days to flag leaf ligule appearance (C and D) and days to anthesis (E and F) for 91 RILs of the Ofanto × Cappelli cross grown in the field in Ottava, Sardinia, Italy during the 2021–2013 growing season (OT2013, circles) and in Foggia, Italy during the 2007–2008 (FO08, triangles) and 2008–2009 (FO09, squares) growing seasons (validation data set). Simulations were performed with the SiriusQuality wheat phenology model using original (A) and QTL-based (B) genetic parameters. Final leaf number and days to flag leaf ligule appearance were recorded in OT2013 only. Inset panels in (E) and (F) show the mean values for the three field experiments. Days to flag leaf ligule and anthesis were calculated from the day after sowing. Dashed lines are 1:1 lines, solid lines are linear regression. Measurements are the mean ± 1 s.d. for $n = 3$ independent replicates.

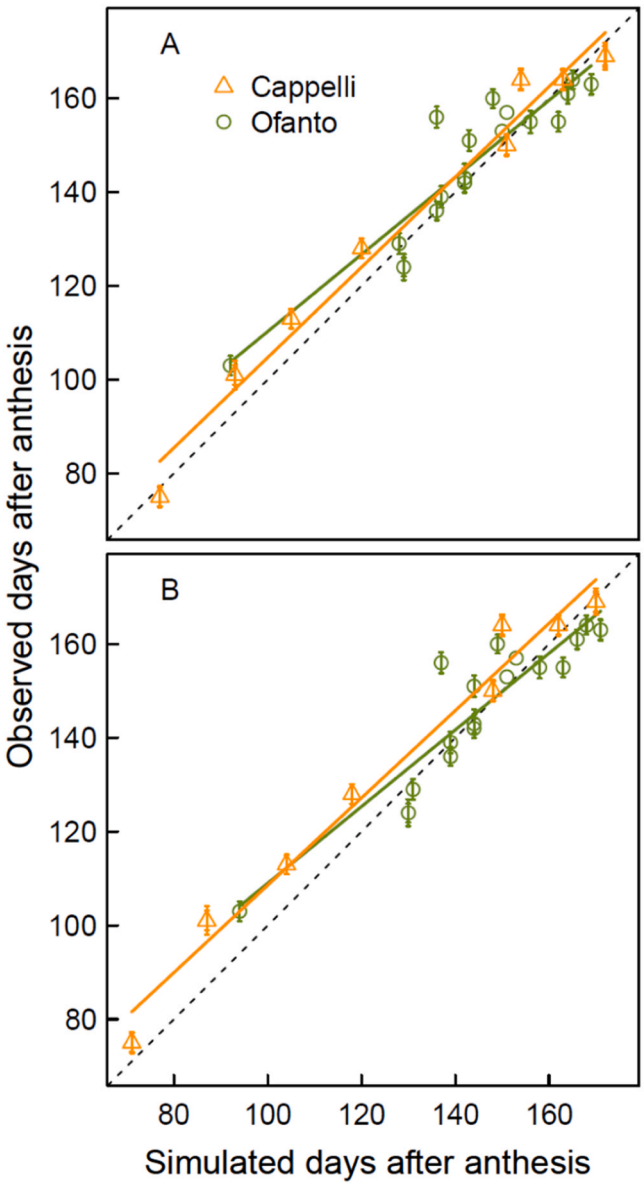

Fig. 7. Simulated versus observed days to anthesis for the two parents grown in the field in 18 (Cappelli) and eight (Ofanto) site/year/sowing date combinations. Simulations were performed with the wheat model *SiriusQuality* using the original (A) and QTL-based (B) parameters. Days to flag leaf ligule and anthesis were calculated from the day after sowing. Dashed lines are 1:1 lines, solids lines are linear regression. Measurements are the mean ± 1 s.d. for $n = 3$ independent replicates.

date of the RIL population, including the parents, which were not used for QTL identification, in untested environments in the field. We discuss the approach we used to estimate the parameters of the model and their association with QTL and major phenology genes that collocate at QTL.

4.1. Genotypic parameters for earliness per se, cold requirement, and photoperiod sensitivity can be estimated independently with vernalization and photoperiod treatments

We estimated five genotypic parameters independently for earliness *per se*, cold requirement, and photoperiod sensitivity using three vernalization and photoperiod treatments. This procedure minimized the risk of finding local minima and reduced the computation time for parameter estimation. It increases the risk of compensation for errors, but it is a better test of the model compared with the estimation of all parameters together.

For the validation data set, the RMSE for anthesis date was low and was similar for the model with estimated parameters (2.0 d RMSE) and with QTL-based parameters (2.5 d RMSE). Compared with previous studies, the RMSE for anthesis date, was lower than that reported for wheat (5–8.6 d in Bogard et al. (2014); 6–9 d in White et al. (2008); 4.3 d in Zheng et al. (2013)) or other species (5–7.5 d in Messina et al. (2006) for soybean; 7.6–15 d in Uptmoor et al. (2012) for Brassica oleracea; 4.2 d in Uptmoor et al. (2017) for spring barley). As in all these studies, we found a significant decrease of the percentage of genetic variations explained with the QTL-based parameters (34 %) compared with the estimated original parameters (56 %). The ranking of the lines for the time to anthesis was better conserved than the r^2, the Spearman's rank correlation coefficient was 0.76 with the estimated parameters and 0.59 with the QTL-based parameters. The lower performance of gene- or QTL-based models can be due to undetected effects of minor QTL (Yin et al., 2005), poor estimation of allelic effects of known QTL (Uptmoor et al., 2012), the use of markers outside the causal polymorphism and possible recombination between markers in linkage disequilibrium (Bogard et al., 2014), or the method used to estimate the QTL or gene parameters (Zheng et al., 2013), in addition to the errors and limitations of the model itself. The fact that the model used in this study does not explicitly consider the effect of DL on *P* and PFLLAnth may explain the low correlation between estimated and QTL-based values for these two parameters, which likely contributed to the lower performance of the QTL-based model.

Bogard et al. (2014), calibrated an empirical phenology model modified from Weir et al. (1984) for a panel of 210 bread wheat genotypes. They estimated the parameters of their model using heading date data from field trials sown in the autumn and spring for the winter and spring type genotypes, respectively. For the winter type genotypes, they found several combinations of parameters that gave similar simulation results for anthesis date and the overall (for spring and winter types) RMSE for heading date was on average two-folds higher for the spring than for the autumn sowings. He et al. (2012) calibrated the model used here for 16 winter wheat cultivars with field data form autumn sown crops and concluded that VAI cannot be estimated using only autumn-sown field trials, even with a large number of environments with a wide range of winter temperature and latitude (daylength). These studies clearly indicate that to estimate vernalization parameters, vernalization and DL treatments are needed, either in the field or under controlled conditions, as used in this study and in previous studies (e.g. Yin et al., 2005; Zheng et al., 2013). Here we show that a minimum of three treatments is required to estimate the three components of phenology.

The treatments should allow for a complete satisfaction of cold requirement of all the studied genotypes. In our study, in the long day vernalized treatments L_f varied between 7.8 and 11.3 leaves among the lines, while the minimum number of leaves of fully vernalized spring wheat genotypes is close to 6 leaves (Levy and Peterson, 1972). L_{min}^{abs} was thus likely overestimated because at least some lines were not fully vernalized in the SDV treatment. This may explain the negative correlation we found between L_{min}^{abs} and SLDL and the five common non-significant QTL for these two parameters. This hypothesis is also supported by the colocation of QTL32 for L_{min}^{abs} at *Vrn-A2*. *VRN2* is a floral repressor expressed only under long days, where it delays flowering until plants are vernalized by repressing *VRN3* (Trevaskis et al., 2007). During cold periods the induction of *VRN1* represses *VRN2*, allowing the day-length response (Yan et al., 2004). Therefore, the colocation of QTL32 for L_{min}^{abs} at *Vrn-A2* can be explained by admitting that the vernalization treatment in the SDV treatments resulted in some lines being not fully vernalized.

4.2. High-throughput field phenotyping for estimating model parameters in large genetic populations

We used twice-weekly measurements of Haun stage, final main stem leaf number, and anthesis date of long-day vernalized plants to estimate the three earliness *per se* parameters (L_{min}^{abs}, *P*, and, PFLLAnth), while the rate of vernalization (VAI) and the sensitivity to DL (SLDLL) were estimated using observations of the date of flag leaf ligule appearance of nonvernalized plants grown under long days (LDNV) and vernalized plants grown under short days (SDV), respectively. SLDL and VAI were estimated by minimizing the error for the date of flag leaf ligule appearance rather than for L_f to reduce the compensation for error for PFLLAnth. It also improved the simulation of the stage flag leaf ligule just visible, which is synchronous with the stage male meiosis, a key stage to model the impact of abiotic stress on grain number abortion (Barber et al., 2015).

Depending on the objectives of the study, our phenotyping protocol can be greatly simplified to phenotype larger size genetic populations. The minimum information required to calibrate the model are the Haun stage measured every about two to three leaves and anthesis or heading date (Jamieson and Munro, 2000) for the three treatments used in this study. These treatments can be applied in single-row nurseries in the field where daylength can be extended by spring sowing (as in this study) or by the use of artificial lights (Zheng et al., 2013). Compared with the classical approach, which uses multi-year and multi-site field trials, our approach requires much less environments, as the three treatments can be done in a single growing season on a single location. Coupled with high-throughput phenotyping methods our approach is thus much faster and can be applied to large genetic populations.

With the rapid development of plant phenomics, all the measurements required to calibrate the model for new genotypes can be automatized at high throughput. Methods using high-resolution visible imagery with deep-learning algorithms have been developed to estimate the date of heading and anthesis (Sadeghi-Tehran et al., 2017; Velumani et al., 2020) and leaf tip number, and thus *P* (Li et al., 2023). Methods have also recently been developed for high throughput phenotyping of the date of flag leaf ligule appearance (S. Liu personal communication). These phenomics methods will greatly facilitate the calibration of the model used in this study for large genetic panels for genetic analyses and breeding, which currently is the bottleneck of our approach.

4.3. Model parameters are to a large extent genetically independent and are associated with major phenology genes

We predicted the parameter values considering only the additive effect of the QTL but Bogard et al. (2014) found non-significant or small bi-locus marker x marker interactions for markers associated with model parameters for vernalization requirement and photoperiod in the bread wheat panel they studied. Our objective was not to identify robust QTL but to predict the genetic value of parameters; therefore, we used all available information and predicted the parameters using all (tentative) QTL with a LOD score > 1.

The multi-linear models predicted the five genotypic parameters with six to 11 QTL and explained 36–68 % of the genetic variation of the estimated parameters. In comparison, Bogard et al. (2014) estimated three model parameters and their multi-linear predictions based markers explained 68–71 % of the variation of their parameter. Recombinations between markers may be the cause of the large part of the genetic variation of the parameter not explained by the QTL in our study. The remaining unexplained variations of the parameters may be due to QTL with smaller effect that were not detected because of the limited size of our population and insufficient coverage of the genetic map.

Twenty-nine of the 30 QTL used to predict the parameters colocalized with known phenology QTL. Our study provides a quantification of their effect that is independent of the environment that can be used to predict the phenology of genotypes in different environments. They also provide new insights onto the physiological processes controlled by the associated regions. Twelve of the 13 major and moderate QTL we identified were associated with only one parameter and several collocated at major phenology (Vrn-A1, Vrn-A2, Vrn-B3, Pppd-B1, CO-2, and FT-A5), reflecting that the parameters are genetically independent for the most part and that the model discriminates well the effect of the physiological processes controlling the phenological development of wheat.

PFFLAnth had a relatively high standard deviation between lines (0.28 phyllochron) but a low heritability (8.7 %) and we found no significant QTL for this parameter. A previous study on the same population also did not find any significant QTL for the duration in thermal time between flag leaf ligule appearance and anthesis (Sanna et al., 2014). It has been reported that this period is sensitive to DL (Fischer, 2011; Whitechurch et al., 2007). Here, PFFLAnth was significantly correlated with *P* and SLDL (Fig. 1). These correlations were, at least in part, due to the nature of these parameters and the way they were estimated. *P* and SLDL directly depend on the rate of leaf appearance, and PFLLAnth is expressed in phyllochronic time. The impact of a different rate of leaf appearance induced by DL is mediated by the number of plastochrons that the plant is able to produce and by the variation in duration induced by photoperiod. Improving the prediction of the duration of the phase between flag leaf appearance and anthesis (that is PFFLAnth) is an important model improvement target as it has a strong effect on grain number per ear (Fischer, 2011).

In contrast with major and moderate QTL, half of the tentative QTL were associated with two to four parameters (Fig. 8). Four of these QTL, and the tentative QTL28, were associated with L_{min}^{abs} and SLDL. At least some of these QTL colocations are likely related to incomplete vernalization of some lines in LDV treatment (e.g. the common QTL between PFLLANTh and VAI). SLDL and *P* were significantly correlated ($r = 0.40$, $P = 0.001$) and we found two tentative QTL (QTL10 and QTL27) associated with these two parameters (Figs. 3 and 8). In winter barley, under long days conditions genotypes carrying the photoperiod sensitive

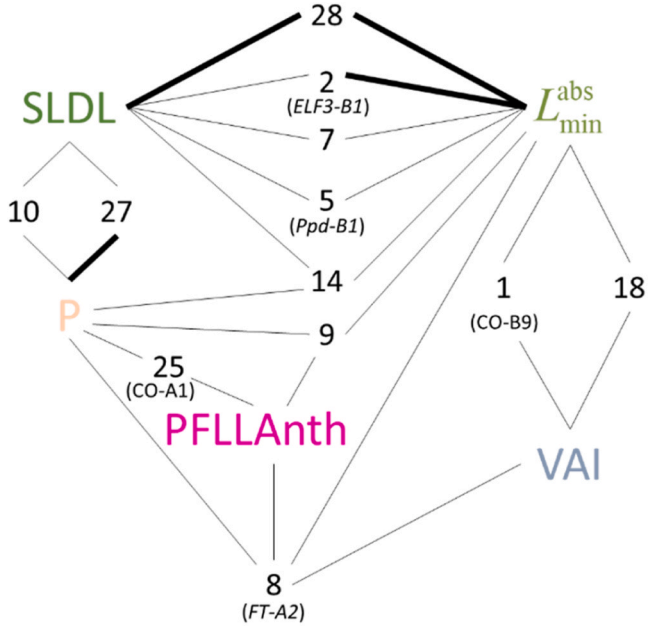

Fig. 8. Schema of the QTL associated with two or more model parameters. Tick lines are major and moderate QTL with LOD > 2.8 and thin lines are tentative QTL with LOD between 1.0. and 2.8. Numbers correspond to the QTL numbers in Table 2 and in Fig. 3. Parameters are defined in Table 1. Major phenology genes that collocate at QTL are indicated under the QTL numbers.

alleles of *Ppd1-H1* (early flowering) have a reduced leaf length and an higher leaf appearance rate (Digel et al., 2016). In wheat, the DL insensitivity alleles of *Ppd-1* was also found to reduce phyllochron under long day in the field but only after leaf 7 (Ochagavía et al., 2017), confirming the effect of photoperiod on the rate of emergence of late-formed leaves found by Miralles and Richards (2000). In agreement with these results, QTL10 and QTL27 had opposite additive effects on SLDL and *P*. These results suggest the opportunity to consider an effect of DL sensitivity on *P*. Although expressed only for the last leaves, this would modify the duration of the terminal spikelet to anthesis and flag leaf appearance to anthesis periods. Although none of the mentioned QTL collocated at *Ppd-1*, they may carry genes down- or up-stream of *Ppd-1*. However, the common genetic determinism of *P* and SLDL need to be further studied as we cannot rule out that it can be driven by carbon limitations during the stem extension period (Baumont et al., 2019).

Even though several studies reported epistatic interactions between major phenology genes, including for wheat, the advantage of including epistatic interactions in QTL-based models is still questionable. Bogard et al. (2014) did not find any significant improvement in the simulation of heading date following the inclusion of epistatic interactions in their QTL-based model. This may be rooted in the nature of process-based models. Biological epistatic interactions can occur when a process (e.g. anthesis date) is the product of two or more processes (e.g. vernalization and photoperiod response) at a lower the level of organization (Holland, 2001; Melchinger et al., 1994). Multiplicative interactions are a special case of epistasis that, in some cases, can results from additive gene effect (Holland, 2001). Although there is limited evidence in the literature, epistatic interactions in process-based models are not necessarily limited to multiplicative interactions (Hammer et al., 2019). By explicitly modeling the (non)-linear relationships among traits, ecophysiological models have the potential to account for biologic epistatic effects (Technow et al., 2015). In this work, epistatic interactions were not explicitly considered in the QTL detection, nor in the genetic models of the parameters of the model, but the model has the potential to consider epistatic interactions by considering complex relationships between biological processes. Some of the colocations between model parameters schematized in Fig. 8 illustrate putative epistatic interactions between model parameters.

5. Conclusion

The QTL-based model of phenology developed in this study gives the possibility to quantify the effect of major phenology genes on agronomically important traits that are to a large part determined by phenology (e.g. cold hardness, tillering, leaf size, plant height, and grain number per ear; Hyles et al. (2020) in diverse environments. Future work should further evaluate the QTL-based model under more divers environments and for different genetic populations. This would provide a better understanding of the model's performance and applicability in different contexts.

In contrast with empirical models that simulate thermal times between phenological states, the model used in this study simulates key developmental stages (floral initiation, terminal spikelets, flag leaf tip and ligule appearance) that define phase switch changes in leaf area (Martre and Dambreville, 2018), tillering (Abichou et al., 2018), and spikelet production and floret abortion (González et al., 2011). Future model development should consider the rate and duration of the phases of spikelet primordium formation and floret development, which are controlled by flowering time regulators (Gol et al., 2017), and determine the number spikelet per ear and floret survival and abortion (González et al., 2011). Kirby (1990) showed that the rate of spikelet primordium formation is directly related to L_f. In this study, we identified four major QTL for three parameters (*P*, SLDL, and L_{min}^{abs}) that colocalized with known QTL for spikelet number per ear (Table 2). Future studies with the model used in this study should also try to use makers in the causal polymorphism of known major phenology genes. This will provide quantitative information on the effect of this genes on important physiological traits (model parameters).

CRediT authorship contribution statement

Pasquale De Vita: Writing – review & editing, Data curation. **Francesco Giunta:** Writing – review & editing, Investigation, Conceptualization. **Anna Mastrangelo:** Writing – review & editing, Investigation. **Daniela Marone:** Writing – review & editing, Investigation. **Pierre Martre:** Writing – original draft, Visualization, Software, Formal analysis, Conceptualization. **Rosella Motzo:** Writing – review & editing, Investigation, Data curation.

Declaration of Competing Interest

The authors declare that they have no known competing financial interests or personal relationships that could have appeared to influence the work reported in this paper.

Data availability

Data will be made available on request.

Acknowledgements

PM acknowledges the support of the University of Sassari during his stays to conduct this research through its 2020 visiting Professor program funded by the Regional Government of Sardinia, and Dr. Renaud Rincent (UMR GQE, INRAE, France) for helpful discussions.

Appendix A

Table A1
List of symbols and their description.

Symbol	Description
DL	Daylength
FO08	Experiment conducted in Foggia during the 2007–2008 growing season
FO09	Experiment conducted in Foggia during the 2008–2009 growing season
G x E	Genotype x environnement interaction
L_f	Final main-stem leaf number
LC	Lack of correlation
LDNV	Long days nonvernalized treatment
LDV	Long days vernalized treatment

(*continued on next page*)

Table A1 (*continued*)

Symbol	Description
LOD	Logarithm of odds
NU	Non-unity slope
OT13	Experiment conducted in Ottava during the 2012–2013 growing season
P	Phyllochron
QTL	Quantitative trait loci
r^2	Coefficient of determination
RIL	Recombinant inbreed line
RMSE	Root mean squared error
SB	Squared bias
SD	Sowing date in day of the year
$SD_{W/S}$	Sowing dates for which P_{SD} is minimum
$SD_{S/A}$	Sowing dates for which P_{SD} is maximum
SDV	Short days vernalized treatment
T_t	Thermal time since plant emergence
ρ	Spearman's rank correlation coefficient

Appendix B. Supporting information

Supplementary data associated with this article can be found in the online version at doi:10.1016/j.eja.2024.127379.

References

Abichou, M., Fournier, C., Dornbusch, T., Chambon, C., de Solan, B., Gouache, D., Andrieu, B., 2018. Parameterising wheat leaf and tiller dynamics for faithful reconstruction of wheat plants by structural plant models. Field Crops Res. 218, 213–230. https://doi.org/10.1016/j.fcr.2018.01.010.

Allard, V., Veisz, O., Kőszegi, B., Rousset, M., Le Gouis, J., Martre, P., 2012. The quantitative response of wheat vernalization to environmental variables indicates that vernalization is not a response to cold temperature. J. Exp. Bot. 63 (2), 847–857.

Asseng, S., Martre, P., Maiorano, A., Rötter, R.P., O'Leary, G.J., Fitzgerald, G.J., Girousse, C., Motzo, R., Giunta, F., Babar, M.A., Reynolds, M.P., Kheir, A.M.S., Thorburn, P.J., Waha, K., Ruane, A.C., Aggarwal, P.K., Ahmed, M., Balkovič, J., Basso, B., Biernath, C., Bindi, M., Cammarano, D., Challinor, A.J., De Sanctis, G., Dumont, B., Eyshi Rezaei, E., Fereres, E., Ferrise, R., Garcia-Vila, M., Gayler, S., Gao, Y., Horan, H., Hoogenboom, G., Izaurralde, R.C., Jabloun, M., Jones, C.D., Kassie, B.T., Kersebaum, K.-C., Klein, C., Koehler, A.-K., Liu, B., Minoli, S., Montesino San Martin, M., Müller, C., Naresh Kumar, S., Nendel, C., Olesen, J.E., Palosuo, T., Porter, J.R., Priesack, E., Ripoche, D., Semenov, M.A., Stöckle, C., Stratonovitch, P., Streck, T., Supit, I., Tao, F., Van der Velde, M., Wallach, D., Wang, E., Webber, H., Wolf, J., Xiao, L., Zhang, Z., Zhao, Z., Zhu, Y., Ewert, F., 2019. Climate change impact and adaptation for wheat protein. Glob. Chang. Biol. 25 (1), 155–173. https://doi.org/10.1111/gcb.14481.

Barber, H.M., Carney, J., Alghabari, F., Gooding, M.J., 2015. Decimal growth stages for precision wheat production in changing environments? Ann. Appl. Biol. 166 (3), 355–371. https://doi.org/10.1111/aab.12207.

Baumont, M., Parent, B., Manceau, L., Brown, H.E., Driever, S.M., Muller, B., Martre, P., 2019. Experimental and modeling evidence of carbon limitation of leaf appearance rate for spring and winter wheat. J. Exp. Bot. 70 (9), 2449–2462. https://doi.org/10.1093/jxb/erz012.

Bertin, N., Martre, P., Genard, M., Quilot, B., Salon, C., 2010. Under what circumstances can process-based simulation models link genotype to phenotype for complex traits? Case-study of fruit and grain quality traits. J. Exp. Bot. 61 (4), 955–967. https://doi.org/10.1093/jxb/erp377.

Bogard, M., Biddulph, B., Zheng, B., Hayden, M., Kuchel, H., Mullan, D., Allard, V., Le Gouis, J., Chapman, S.C., 2020a. Linking genetic maps and simulation to optimize breeding for wheat flowering time in current and future climates. Crop Sci. 60 (2), 678–699. https://doi.org/10.1002/csc2.20113.

Bogard, M., Hourcade, D., Piquemal, B., Gouache, D., Deswartes, J.-C., Throude, M., Cohan, J.-P., 2020b. Marker-based crop model-assisted ideotype design to improve avoidance of abiotic stress in bread wheat. J. Exp. Bot. 72 (4), 1085–1103. https://doi.org/10.1093/jxb/eraa477.

Bogard, M., Ravel, C., Paux, E., Bordes, J., Balfourier, F., Chapman, S.C., Le Gouis, J., Allard, V., 2014. Predictions of heading date in bread wheat (*Triticum aestivum* L.) using QTL-based parameters of an ecophysiological model. J. Exp. Bot. 65 (20), 5849–5865. https://doi.org/10.1093/jxb/eru328.

Brent, R.P., 1973. Algorithms for minimization without derivatives. Prentice-Hall, Englewood Cliffs, New Jersey.

Brooking, I.R., Jamieson, P.D., Porter, J.R., 1995. The influence of daylength on final leaf number in spring wheat. Field Crops Res 41, 155–165.

Brooking, I.R., Jamieson, P.D., 2002. Temperature and photoperiod response of vernalization in near-isogenic lines of wheat. Field Crops Res 79 (1), 21–38.

Brown, H.E., Jamieson, P.D., Brooking, I.R., Moot, D.J., Huth, N.I., 2013. Integration of molecular and physiological models to explain time of anthesis in wheat. Ann. Bot. 112 (9), 1683–1703. https://doi.org/10.1093/aob/mct224.

Buerstmayr, M., Huber, K., Heckmann, J., Steiner, B., Nelson, J.C., Buerstmayr, H., 2012. Mapping of QTL for Fusarium head blight resistance and morphological and developmental traits in three backcross populations derived from *Triticum dicoccum* × *gib*. Theor. Appl. Genet. 125 (8), 1751–1765. https://doi.org/10.1007/s00122-012-1951-2.

Chenu, K., Chapman, S.C., Tardieu, F., McLean, G., Welcker, C., Hammer, G.L., 2009. Simulating the yield impacts of organ-level quantitative trait loci associated with drought response in maize: A "gene-to-phenotype" modeling approach. Genetics 183 (4), 1507–1523. https://doi.org/10.1534/genetics.109.105429.

Darvasi, A., Soller, M., 1997. A simple method to calculate resolving power and confidence interval of QTL map location. Behav. Genet. 27 (2), 125–132. https://doi.org/10.1023/a:1025685324830.

Digel, B., Tavakol, E., Verderio, G., Tondelli, A., Xu, X., Cattivelli, L., Rossini, L., von Korff, M., 2016. Photoperiod1 (Ppd-H1) controls leaf size. Plant Physiol. 172, 405–415. https://doi.org/10.1104/pp.16.00977.

Donatelli, M., Rizzoli, A.E., 2008. A design for framework-independent model components of biophysical systems. In: Sànchez-Marrè, M., Béjar, J., Comas, J., Rizzoli, A., Guariso, G. (Eds.), 4th Biennial Meeting of the International Environmental Modelling and Software Society 2008: International Congress on Environmental Modelling and Software. Universitat Politècnica de Catalunya, Barcelona, Catalonia, pp. 727–734.

Dornbusch, T., Baccar, R., Watt, J., Hillier, J., Bertheloot, J., Fournier, C., Andrieu, B., 2011. Plasticity of winter wheat modulated by sowing date, plant population density and nitrogen fertilisation: dimensions and size of leaf blades, sheaths and internodes in relation to their position on a stem. Field Crops Res 121 (1), 116–124. https://doi.org/10.1016/j.fcr.2010.12.004.

Dubcovsky, J., Loukoianov, A., Fu, D., Valarik, M., Sanchez, A., Yan, L., 2006. Effect of photoperiod on the regulation of wheat vernalization genes VRN1 and VRN2. Plant Mol. Biol. 60 (4), 469–480. https://doi.org/10.1007/s11103-005-4814-2.

Evans, L., 1987. Short day induction of inflorescence initiation in some winter wheat varieties. Aust. J. Plant Physiol. 14, 277–286.

Fischer, R.A., 2011. Wheat physiology: a review of recent developments. Crop Pasture Sci. 62 (2), 95–114. https://doi.org/10.1071/CP10344.

Fischer, R.A., 2016. The effect of duration of the vegetative phase in irrigated semi-dwarf spring wheat on phenology, growth and potential yield across sowing dates at low latitude. Field Crops Res 198, 188–199. https://doi.org/10.1016/j.fcr.2016.06.019.

Gauch, H.G., Hwang, J.T.G., Fick, G.W., 2003. Model evaluation by comparison of model-based predictions and measured values. Agron. J. 95 (6), 1442–1446.

Giraldo, P., Royo, C., González, M., Carrillo, J.M., Ruiz, M., 2016. Genetic diversity and association mapping for agromorphological and grain quality traits of a structured collection of durum wheat landraces igiunncluding subsp. durum, turgidum and diccocon. PLOS ONE 11 (11), e0166577. https://doi.org/10.1371/journal.pone.0166577.

Giunta, F., De Vita, P., Mastrangelo, A.M., Sanna, G., Motzo, R., 2018. Environmental and genetic variation for yield-related traits of durum wheat as affected by development. Front Plant Sci. 9, 8. https://doi.org/10.3389/fpls.2018.00008.

Gol, L., Tomé, F., von Korff, M., 2017. Floral transitions in wheat and barley: interactions between photoperiod, abiotic stresses, and nutrient status. J. Exp. Bot. 68 (7), 1399–1410. https://doi.org/10.1093/jxb/erx055.

González, F.G., Miralles, D.J., Slafer, G.A., 2011. Wheat floret survival as related to pre-anthesis spike growth. J. Exp. Bot. 62 (14), 4889–4901. https://doi.org/10.1093/jxb/err182.

Gonzalez-Navarro, O.E., Griffiths, S., Molero, G., Reynolds, M.P., Slafer, G.A., 2016. Variation in developmental patterns among elite wheat lines and relationships with yield, yield components and spike fertility. Field Crops Res. 196, 294–304. https://doi.org/10.1016/j.fcr.2016.07.019.

Griffiths, S., Simmonds, J., Leverington, M., Wang, Y., Fish, L., Sayers, L., Alibert, L., Orford, S., Wingen, L., Herry, L., Faure, S., Laurie, D., Bilham, L., Snape, J., 2009. Meta-QTL analysis of the genetic control of ear emergence in elite European winter

wheat germplasm. Theor. Appl. Genet. 119 (3), 383–395. https://doi.org/10.1007/s00122-009-1046-x.
Gupta, P., Kabbaj, H., El Hassouni, K., Maccaferri, M., Sanchez-Garcia, M., Tuberosa, R., Bassi, F.M., 2020. Genomic regions associated with the control of flowering time in durum wheat. Plants 9 (12). https://doi.org/10.3390/plants9121628.
Hammer, G., Messina, C., Wu, A., Cooper, M., 2019. Biological reality and parsimony in crop models—why we need both in crop improvement! Silico Plants 1 (1). https://doi.org/10.1093/insilicoplants/diz010.
Hay, R.K.M., Kirby, E.J.M., 1991. Convergence and synchrony-a review of the coordination of development in wheat. Aust. J. Agric. Res. 42 (5), 661–700.
He, J., Le Gouis, J., Stratonovitch, P., Allard, V., Gaju, O., Heumez, E., Orford, S., Griffiths, S., Snape, J.W., Foulkes, M.J., Semenov, M.A., Martre, P., 2012. Simulation of environmental and genotypic variations of final leaf number and anthesis date for wheat. Eur. J. Agron. 42, 22–33. https://doi.org/10.1016/j.eja.2011.11.002.
Holland, J., 2001. Epistasis and plant breeding. Plant Breed. Rev. 21, 27–92. https://doi.org/10.1002/9780470650196.ch2.
Hoogenboom, G., White, J.W., Acosta-Gallegos, J., Gaudiel, R.G., Myers, J.R., Silbernagel, M.J., 1997. Evaluation of a crop simulation model that incorporates gene action. Agron. J. 89, 613–620.
Hoogenboom, G., White, J.W., 2003. Improving physiological assumptions of simulation models by using gene-based approaches. Agron. J. 95, 82–89. https://doi.org/10.2134/agronj2003.8200.
Hyles, J., Bloomfield, M.T., Hunt, J.R., Trethowan, R.M., Trevaskis, B., 2020. Phenology and related traits for wheat adaptation. Heredity 125 (6), 417–430. https://doi.org/10.1038/s41437-020-0320-1.
Jamieson, P.D., Brooking, I.R., Porter, J.R., Wilson, D.R., 1995a. Prediction of leaf appearance in wheat: a question of temperature. Field Crops Res 41, 35–44.
Jamieson, P.D., Brooking, I.R., Semenov, M.A., Porter, J.R., 1998. Making sense of wheat development: a critique of methodology. Field Crops Res. 55 (1/2), 117–127.
Jamieson, P.D., Brooking, I.R., Semenov, M.A., McMaster, G.S., White, J.W., Porter, J.R., 2007. Reconciling alternative models of phenological development in winter wheat. Field Crops Res. 103 (1), 36–41.
Jamieson, P.D., Francis, G.S., Wilson, D.R., Martin, R.J., 1995b. Effects of water deficits on evapotranspiration from barley. Agric. For. Meteorol. 76 (1), 41–58.
Jamieson, P.D., Munro, C.A., 2000. The calibration of a model for daylength responses in spring wheat for large numbers of cultivars. Proc. Agron. Soc. 30, 25–29.
Joehanes, R., Nelson, J.C., 2008. QGene 4.0, an extensible Java QTL-analysis platform. Bioinformatics 24, 2788e2789.
Kirby, E.J.M., 1990. Co-ordination of leaf emergence and leaf and spikelet primordium initiation in wheat. Field Crops Res 25 (3-4), 253–264.
Kiss, T., Dixon, L.E., Soltész, A., Bányai, J., Mayer, M., Balla, K., Allard, V., Galiba, G., Slafer, G.A., Griffiths, S., Veisz, O., Karsai, I., 2017. Effects of ambient temperature in association with photoperiod on phenology and on the expressions of major plant developmental genes in wheat (*Triticum aestivum* L.). Plant Cell Environ. 40 (8), 1629–1642. https://doi.org/10.1111/pce.12971.
Kuchel, H., Hollamby, G., Langridge, P., Williams, K., Jefferies, S.P., 2006. Identification of genetic loci associated with ear-emergence in bread wheat. Theor. Appl. Genet. 113 (6), 1103–1112. https://doi.org/10.1007/s00122-006-0370-7.
Le Gouis, J., Bordes, J., Ravel, C., Heumez, E., Faure, S., Praud, S., Galic, N., Remoue, C., Balfourier, F., Allard, V., Rousset, M., 2012. Genome-wide association analysis to identify chromosomal regions determining components of earliness in wheat. Theor. Appl. Genet. 124 (3), 597–611. https://doi.org/10.1007/s00122-011-1732-3.
Levy, J., Peterson, M.L., 1972. Responses of spring wheats to vernalization and photoperiod. Crop Sci. 12 (4), 487–490. https://doi.org/10.2135/cropsci1972.0011183X001200040029x.
Li, Y., Zhan, X., Liu, S., Lu, H., Jiang, R., Guo, W., Chapman, S., Ge, Y., Solan, B., Ding, Y., Baret, F., 2023. Self-supervised plant phenotyping by combining domain adaptation with 3D plant model simulations: application to wheat leaf counting at seedling stage. Plant Phenomics 5, 0041. https://doi.org/10.34133/plantphenomics.0041.
Maccaferri, M., Cane', M.A., Sanguineti, M.C., Salvi, S., Colalongo, M.C., Massi, A., Clarke, F., Knox, R., Pozniak, C.J., Clarke, J.M., Fahima, T., Dubcovsky, J., Xu, S., Ammar, K., Karsai, I., Vida, G., Tuberosa, R., 2014. A consensus framework map of durum wheat (*Triticum durum* Desf.) suitable for linkage disequilibrium analysis and genome-wide association mapping. BMC Genom. 15 (1), 873. https://doi.org/10.1186/1471-2164-15-873.
Maccaferri, M., Harris, N.S., Twardziok, S.O., Pasam, R.K., Gundlach, H., Spannagl, M., Ormanbekova, D., Lux, T., Prade, V.M., Milner, S.G., Himmelbach, A., Mascher, M., Bagnaresi, P., Faccioli, P., Cozzi, P., Lauria, M., Lazzari, B., Stella, A., Manconi, A., Gnocchi, M., Moscatelli, M., Avni, R., Deek, J., Biyiklioglu, S., Frascaroli, E., Corneti, S., Salvi, S., Sonnante, G., Desiderio, F., Marè, C., Crosatti, C., Mica, E., Özkan, H., Kilian, B., De Vita, P., Marone, D., Joukhadar, R., Mazzucotelli, E., Nigro, D., Gadaleta, A., Chao, S., Faris, J.D., Melo, A.T.O., Pumphrey, M., Pecchioni, N., Milanesi, L., Wiebe, K., Ens, J., MacLachlan, R.P., Clarke, J.M., Sharpe, A.G., Koh, C.S., Liang, K.Y.H., Taylor, G.J., Knox, R., Budak, H., Mastrangelo, A.M., Xu, S.S., Stein, N., Hale, I., Distelfeld, A., Hayden, M.J., Tuberosa, R., Walkowiak, S., Mayer, K.F.X., Ceriotti, A., Pozniak, C.J., Cattivelli, L., 2019. Durum wheat genome highlights past domestication signatures and future improvement targets. Nat. Genet. 51 (5), 885–895. https://doi.org/10.1038/s41588-019-0381-3.
Maccaferri, M., Sanguineti, M.C., Demontis, A., El-Ahmed, A., Garcia del Moral, L., Maalouf, F., Nachit, M., Nserallah, N., Ouabbou, H., Rhouma, S., Royo, C., Villegas, D., Tuberosa, R., 2011. Association mapping in durum wheat grown across a broad range of water regimes. J. Exp. Bot. 62 (2), 409–438. https://doi.org/10.1093/jxb/erq287.
Manceau, L., Martre, P., 2018. SiriusQuality-BioMa-Phenology-Component (Version v1.0.0). Zenodo. https://doi.org/10.5281/zenodo.2478791.
Marcotuli, I., Gadaleta, A., Mangini, G., Signorile, A.M., Zacheo, S.A., Blanco, A., Simeone, R., Colasuonno, P., 2017. Development of a high-density SNP-based linkage map and detection of QTL for beta-glucans, protein content, grain yield per spike and heading time in durum wheat. Int. J. Mol. Sci. 18 (6). https://doi.org/10.3390/ijms18061329.
Marone, D., Panio, G., Ficco, D.M., Russo, M., De Vita, P., Papa, R., Rubiales, D., Cattivelli, L., Mastrangelo, A., 2012. Characterization of wheat DArT markers: genetic and functional features. Mol. Genet Genom. 287 (9), 741–753. https://doi.org/10.1007/s00438-012-0714-8.
Martre, P., Dambreville, A., 2018. A model of leaf coordination to scale-up leaf expansion from the organ to the canopy. Plant Physiol. 176 (1), 704–716. https://doi.org/10.1104/pp.17.00986.
Martre, P., Jamieson, P.D., Semenov, M.A., Zyskowski, R.F., Porter, J.R., Triboi, E., 2006. Modelling protein content and composition in relation to crop nitrogen dynamics for wheat. Eur. J. Agron. 25, 138–154. https://doi.org/10.1016/j.eja.2006.04.007.
Martre, P., Quilot-Turion, B., Luquet, D., Ould-Sidi Memmah, M.-M., Chenu, K., Debaeke, P., 2014. Model-assisted phenotyping and ideotype design. In: Sadras, V., Calderini, D. (Eds.), Crop physiology. Applications for genetic improvemetn and agronomy. Academic Press, London, UK, pp. 323–373.
McMaster, G.S., Wilhelm, W.W., Palic, D.B., Porter, J.R., Jamieson, P.D., 2003. Spring wheat leaf appearance and temperature: extending the paradigm? Ann. Bot. 91, 697–705.
Melchinger, A.E., Singh, M., Link, W., Utz, H., von Kittlitz, E., 1994. Heterosis and gene effects of multiplicative characters: theoretical relationships and experimental results from *Vicia faba* L (https://doi.org/doi). Theor. Appl. Genet 88, 343–348. https://doi.org/10.1007/BF00223643 PMID: 24186017.
Mengistu, D.K., Kidane, Y.G., Catellani, M., Frascaroli, E., Fadda, C., Pè, M.E., Dell'Acqua, M., 2016. High-density molecular characterization and association mapping in Ethiopian durum wheat landraces reveals high diversity and potential for wheat breeding. Plant Biotechnol. J. 14 (9), 1800–1812. https://doi.org/10.1111/pbi.12538.
Messina, C.D., Jones, J.W., Boote, K.J., Vallejos, C.E., 2006. A gene-based model to simulate soybean development and yield responses to environment. Crop Sci. 46 (1), 456–466.
Milner, S.G., Maccaferri, M., Huang, B.E., Mantovani, P., Massi, A., Frascaroli, E., Tuberosa, R., Salvi, S., 2016. A multiparental cross population for mapping QTL for agronomic traits in durum wheat (*Triticum turgidum* ssp. *durum*). Plant Biotechnol. J. 14 (2), 735–748. https://doi.org/10.1111/pbi.12424.
Miralles, D.J., Richards, R.A., 2000. Responses of leaf and tiller emergence and primordium initiation in wheat and barley to interchanged photoperiod. Ann. Bot. 85 (5), 655–663.
Nakagawa, H., Yamagishi, J., Miyamoto, N., M, M., Yano, M., Nemoto, K., 2005. Flowering response of rice to photoperiod and temperature: a QTL analysis using a phenological model. Theor. Appl. Genet. 110 (4), 778–786.
Nishimura, K., Moriyama, R., Katsura, K., Saito, H., Takisawa, R., Kitajima, A., Nakazaki, T., 2018. The early flowering trait of an emmer wheat accession (*Triticum turgidum* L. ssp. *dicoccum*) is associated with the cis-element of the Vrn-A3 locus. Theor. Appl. Genet. 131 (10), 2037–2053. https://doi.org/10.1007/s00122-018-3131-5.
Ochagavía, H., Prieto, P., Savin, R., Griffiths, S., Slafer, G.A., 2017. Duration of developmental phases, and dynamics of leaf appearance and tillering, as affected by source and doses of photoperiod insensitivity alleles in wheat under field conditions. Field Crops Res 214, 45–55. https://doi.org/10.1016/j.fcr.2017.08.015.
Ochagavía, H., Prieto, P., Savin, R., Griffiths, S., Slafer, G., 2018. Dynamics of leaf and spikelet primordia initiation in wheat as affected by Ppd-1a alleles under field conditions. J. Exp. Bot. 69 (10), 2621–2631. https://doi.org/10.1093/jxb/ery104.
Panio, G., Motzo, R., Mastrangelo, A.M., Marone, D., Cattivelli, L., Giunta, F., De Vita, P., 2013. Molecular mapping of stomatal-conductance-related traits in durum wheat (*Triticum turgidum* ssp. *durum*). Ann. Appl. Biol. 162 (2), 258–270. https://doi.org/10.1111/aab.12018.
Parent, B., Leclere, M., Lacube, S., Semenov, M.A., Welcker, C., Martre, P., Tardieu, F., 2018. Maize yields over Europe may increase in spite of climate change, with an appropriate use of the genetic variability of flowering time. Proc. Natl. Acad. Sci. 115 (42), 10642–10647. https://doi.org/10.1073/pnas.1720716115.
Parent, B., Tardieu, F., 2014. Can current crop models be used in the phenotyping era for predicting the genetic variability of yield of plants subjected to drought or high temperature? J. Exp. Bot. 65 (21), 6179–6189. https://doi.org/10.1093/jxb/eru223.
R Core Team, 2022. R: A language and environment for statistical computing. R Foundation for Statistical Computing, Vienna, Austria.
Rincent, R., Kuhn, E., Monod, H., Oury, F.X., Rousset, M., Allard, V., Le Gouis, J., 2017. Optimization of multi-environment trials for genomic selection based on crop models. Theor. Appl. Genet. https://doi.org/10.1007/s00122-017-2922-4.
Robertson, M.J., Brooking, I.R., Ritchie, J.T., 1996. Temperature response of vernalization in wheat: modelling the effect on the final number of mainstem leaves. Ann. Bot. 78, 371–381.
Roncallo, P.F., Akkiraju, P.C., Cervigni, G.L., Echenique, V.C., 2017. QTL mapping and analysis of epistatic interactions for grain yield and yield-related traits in *Triticum turgidum* L. var. *durum*. Euphytica 213 (12), 277. https://doi.org/10.1007/s10681-017-2058-2.
Ruan, Y., Zhang, W., Knox, R.E., Berraies, S., Campbell, H.L., Ragupathy, R., Boyle, K., Polley, B., Henriquez, M.A., Burt, A., Kumar, S., Cuthbert, R.D., Fobert, P.R., Buerstmayr, H., DePauw, R.M., 2020. Characterization of the genetic architecture for fusarium head blight rin durum wheat: the complex association of resistance, flowering time, and height genes. Front Plant Sci. 11, 592064. https://doi.org/10.3389/fpls.2020.592064.

Sadeghi-Tehran, P., Sabermanesh, K., Virlet, N., Hawkesford, M.J., 2017. Automated method to determine two critical growth stages of wheat: heading and flowering. Front. Plant Sci. 8. https://doi.org/10.3389/fpls.2017.00252.

Sanna, G., Giunta, F., Motzo, R., Mastrangelo, A.M., De Vita, P., 2014. Genetic variation for the duration of pre-anthesis development in durum wheat and its interaction with vernalization treatment and photoperiod. J. Exp. Bot. 65 (12), 3177–3188. https://doi.org/10.1093/jxb/eru170.

Slafer, G.A., Rawson, H.M., 1997. Phyllochron in wheat as affected by photoperiod under two temperature regimes. Aust. J. Plant Physiol. 24 (2), 151–158.

Soriano, J.M., Malosetti, M., Rosello, M., Sorrells, M.E., Royo, C., 2017. Dissecting the old Mediterranean durum wheat genetic architecture for phenology, biomass and yield formation by association mapping and QTL meta-analysis. PLoS One 12 (5), e0178290. https://doi.org/10.1371/journal.pone.0178290.

Sukumaran, S., Reynolds, M.P., Sansaloni, C., 2018. Genome-wide association analyses identify QTL hotspots for yield and component traits in durum wheat grown under yield potential, drought, and heat stress environments. Front. Plant Sci. 9. https://doi.org/10.3389/fpls.2018.00081.

Technow, F., Messina, C.D., Totir, L.R., Cooper, M., 2015. Integrating growth models with whole genome prediction through approximate bayesian computation. PLoS ONE 10 (6), e0130855. https://doi.org/10.1371/journal.pone.0130855.

Trevaskis, B., Hemming, M.N., Dennis, E.S., Peacock, W.J., 2007. The molecular basis of vernalization-induced flowering in cereals. Trends Plant Sci. 12 (8), 352–357.

Uptmoor, R., Li, J., Schrag, T., Stützel, H., 2012. Prediction of flowering time in *Brassica oleracea* using a quantitative trait loci-based phenology model. Plant Biol. 14 (1), 179–189. https://doi.org/10.1111/j.1438-8677.2011.00478.x.

Uptmoor, R., Pillen, K., Matschegewski, C., 2017. Combining genome-wide prediction and a phenology model to simulate heading date in spring barley. Field Crops Res. 202, 84–93. https://doi.org/10.1016/j.fcr.2016.08.006.

Velumani, K., Madec, S., de Solan, B., Lopez-Lozano, R., Gillet, J., Labrosse, J., Jezequel, S., Comar, A., Baret, F., 2020. An automatic method based on daily in situ images and deep learning to date wheat heading stage. Field Crops Res 252, 107793. https://doi.org/10.1016/j.fcr.2020.107793.

Verlotta, A., De Simone, V., Mastrangelo, A., Cattivelli, L., Papa, R., Trono, D., 2010. Insight into durum wheat Lpx-B1: a small gene family coding for the lipoxygenase responsible for carotenoid bleaching in mature grains. BMC Plant Biol. 10 (1), 263.

Voorrips, R.E., 2002. MapChart: software for the graphical presentation of linkage maps and QTLs. J. Herdity 93 (1), 77–78.

Weir, A.H., Bragg, P.L., Porter, J.R., Rayner, J.H., 1984. A winter wheat crop simulation model without water or nutrient limitations. J. Agric. Sci. 102, 371–382.

White, J.W., Herndl, M., Hunt, L.A., Payne, T.S., Hoogenboom, G., 2008. Simulation-based analysis of effects of Vrn and Ppd loci on flowering in wheat. Crop Sci. 48 (2), 678–687. https://doi.org/10.2135/cropsci2007.06.0318.

Whitechurch, E.M., Slafer, G.A., Miralles, D.J., 2007. Variability in the duration of stem elongation in wheat and barley genotypes. J. Agron. Crop Sci. 193 (2), 138–145. https://doi.org/10.1111/j.1439-037X.2007.00260.x.

Wright, T.I.C., Burnett, A.C., Griffiths, H., Kadner, M., Powell, J.S., Oliveira, H.R., Leigh, F.J., 2020. Identification of quantitative trait loci relating to flowering time, flag leaf and awn characteristics in a novel *Triticum dicoccum* mapping population. Plants 9 (7). https://doi.org/10.3390/plants9070829.

Xiong, W., Reynolds, M.P., Crossa, J., Schulthess, U., Sonder, K., Montes, C., Addimando, N., Singh, R.P., Ammar, K., Gerard, B., Payne, T., 2021. Increased ranking change in wheat breeding under climate change. Nat. Plant. 7 (9), 1207–1212. https://doi.org/10.1038/s41477-021-00988-w.

Yan, L., Loukoianov, A., Blechl, A., Tranquilli, G., Ramakrishna, W., SanMiguel, P., Bennetzen, J.L., Echenique, V., Dubcovsky, J., 2004. The wheat VRN2 gene is a flowering repressor down-regulated by vernalization. Science 303 (5664), 1640–1644. https://doi.org/10.1126/science.1094305.

Yin, X., Struik, P.C., van Eeuwijk, F.A., Stam, P., Tang, J., 2005. QTL analysis and QTL-based prediction of flowering phenology in recombinant inbred lines of barley. J. Exp. Bot. 56 (413), 967–976.

Zadoks, J.C., Chang, T.T., Konzak, C.F., 1974. A decimal code for the growth stages of cereals. Weed Res. 14 (6), 415–421. https://doi.org/10.1111/j.1365-3180.1974.tb01084.x.

Zeng, Z., 1994. Precision mapping of quantitative trait loci. Genetics 136, 1457–1468.

Zheng, B., Biddulph, B., Li, D., Kuchel, H., Chapman, S., 2013. Quantification of the effects of VRN1 and Ppd-D1 to predict spring wheat (*Triticum aestivum*) heading time across diverse environments. J. Exp. Bot. 64 (12), 3747–3761. https://doi.org/10.1093/jxb/ert209.

Zheng, B., Chenu, K., Chapman, S.C., 2016. Velocity of temperature and flowering time in wheat – assisting breeders to keep pace with climate change. Glob. Chang. Biol. 22 (2), 921–933. https://doi.org/10.1111/gcb.13118.